AIMS Mathematics, 11(2): 4335–4368.
DOI: 10.3934/math.2026174
Received: 11 November 2025
Revised: 02 February 2026
Accepted: 04 February 2026
Published: 12 February 2026

https://www.aimspress.com/journal/Math

Research article

Study on stability and information sharing sensitivity in blockchain diffusion dynamics with the fractional-order delayed SEIR model

Peng Wan[1], Shujian Ma[1,2], Yuaoran Liu[3], Jiangwen Ju[1], Sumei Pan[4], Jun Wang[1,*] and Minyi Xu[5,*]

[1] School of Mathematical and Physical Sciences, Nanjing Tech University, Nanjing, 211816, China
[2] Institute of Block Chain and Complex Systems, Nanjing Tech University, Nanjing, 211816, China
[3] Institute of Finance and Technology, University College London, 66-72 Gower Street, London WC1E 6EA, United Kingdom
[4] School of Economics and Management, Nanjing Tech University, Nanjing, 211816, China
[5] Nanjing Vocational Institute of Railway Technology, Nanjing, 210031, China

* **Correspondence:** Email: jwang@njtech.edu.cn, 643957163@qq.com.

Abstract: In this study, we tackled the issue of insufficient information sharing among small and medium-sized enterprises (SMEs) in supply chain finance (SCF). Blockchain technology (BCT), with its tamper-proof and decentralized nature, offers a viable solution. The adoption of BCT can be viewed as a diffusion process, which we modeled by extending the classic SEIR epidemic framework with Caputo fractional-order derivatives and time-delay effects. We also introduced a nonlinear index to measure potential adopters' sensitivity to information sharing and examined its influence on diffusion speed and adoption scale. Theoretical analysis showed that when the basic reproduction number exceeds one, a unique endemic equilibrium emerges. Moreover, the interplay between time delays and fractional-order memory effects can trigger Hopf bifurcation, leading to oscillatory adoption patterns. Numerical simulations revealed a negative correlation between the fractional order and critical time delay. Importantly, while greater sensitivity to information sharing generally accelerates diffusion and enlarges the final adoption scale under certain conditions, exceeding an optimal threshold may reduce diffusion efficiency. These results suggest that although enhanced information sharing fosters blockchain adoption, it must be carefully managed to avoid adverse outcomes. This study offers theoretical insights and practical guidance for optimizing blockchain promotion strategies in SCF.

Keywords: supply chain finance; blockchain technology diffusion; fractional-order delayed SEIR model; information sharing sensitivity; stability analysis
Mathematics Subject Classification: 91G45, 34D20, 34K37

Nomenclature

The notation used in this paper is as follows (Table 1).

Table 1. Notation.

Notations	Meaning
$S(t)$	Number of enterprises exposed to BCT but not yet adopted at time t.
$E(t)$	Number of enterprises considering BCT adoption at time t.
$I(t)$	Number of enterprises adopting BCT and integrated into the platform at time t.
$R(t)$	Number of enterprises delisted due to contractual breaches at time t.
Λ	The annual rate of new enterprises entry into the supply chain.
β	Diffusion rate of BCT between enterprises and core adopters.
ε	Transition rate from potential adopting to adopting enterprises.
γ	Rate of enterprise exit from the blockchain platform.
μ	Annual enterprise bankruptcy rate.
τ	Evaluation period: Time required for potential adopters to transition to adopters.
p	Sensitivity of potential adopting enterprises to information sharing.
D_t^α	Caputo fractional derivative.
R_0	Basic reproduction number, measuring the average contagion capability of BCT adoption.
ϑ	The attenuation rate of adoption density.
$C_{\min}$	The diffusion speed of BCT.
$\mathcal{F}$	The final adoption scale of BCT.

The units corresponding to these symbols are provided in Section 4.

1. Introduction

Small and medium-sized enterprises (SMEs) play a crucial role in national economic and social development. According to the World Bank, SMEs account for approximately 90% of all businesses and provide more than half of global employment opportunities [1]. Despite their significance, SMEs often face financing constraints due to low credit ratings and high default risks, and these constraints hinder their growth and development [2]. The emergence of supply chain finance (SCF) has provided a promising solution to these challenges. Under a trade-based credit guarantee model, core enterprises in the supply chain offer guarantees for their partners, enabling SMEs to access loans from financial institutions or fintech companies [3]. However, the multi-tier structure of supply chains frequently results in insufficient information sharing and data transmission barriers between SMEs and core enterprises, perpetuating persistent challenges in SCF [4]. Inadequate information sharing in SCF remains a fundamental barrier to financial efficiency and risk mitigation. As highlighted by Erik Hofmann et al., insufficient information exchange between core enterprises and SMEs directly increases financing costs and limits credit access [5]. From the perspective of transaction cost economics, this inadequacy often arises from concerns over data privacy, the need to protect competitive advantages, the pursuit of additional benefits, the desire for better pricing, the maintenance of bargaining power, and the avoidance of control or oversight from other parties [6–8]. SMEs

frequently struggle to provide verifiable transaction records, further exacerbating trust deficits with financial institutions [9]. Guo Fang Qiu et al. analyzed principal–agent relationships and information asymmetries between entities and commercial banks, examining the associated risks in SCF through the dimensions of risk types, behaviors, and losses [10]. Within the context of inadequate information sharing between upstream and downstream firms in a closed-loop supply chain system, Minghui Ni et al. investigated the effects of corporate social responsibility investments on recycling decisions [11]. Similarly, Abdulaziz et al. explored factors influencing information-sharing inadequacies in agri-food supply chains, including cost-effectiveness, digitalization, environmental context, and process and quality management measures [12]. In summary, inadequate information sharing is pervasive in SCF, impeding the effective transmission of core enterprises' credit to multi-tier suppliers. To address these challenges, digital technologies, particularly blockchain, have emerged as promising solutions.

Blockchain, as a distributed ledger technology driving digital transformation, is characterized by tamper-proof security, decentralization, smart contracts, and consensus mechanisms [4]. These features align closely with the operational needs of modern supply chains. By operating on a decentralized network without a single point of control, blockchain enables all participants to access verified, real-time data on an equal basis. This reduces dependence on central authorities, enhances trust among stakeholders, and mitigates risks arising from inadequate information sharing [6, 13]. Enhanced information sharing, in turn, fosters greater mutual understanding among supply chain partners, thereby improving transparency and operational efficiency [14]. For instance, Samuel Shuai Liu et al. developed a supply chain model comprising a manufacturer and a retailer to analyze blockchain's impact on alleviating information-sharing deficiencies from two dimensions [15]. Lingling Guo et al. proposed an information management framework that integrates blockchain technology (BCT) with the Internet of Things to address information-sharing challenges in SCF transactions [16]. Saberi et al. demonstrated that blockchain enhances traceability and trust through tamper-proof data sharing, although they noted that finance-specific adoption requires stronger interoperability standard [17]. Similarly, Tsan-Ming Choi identified blockchain and IoT as solutions for transparency, but observed that implementation has progressed slowly [18]. Researchers, including Saberi and Choi, have attributed this slow adoption to multiple complex factors. Kumar et al. further investigated how blockchain influences users' willingness to share information regarding blockchain-enabled technological products. Their study shows that while blockchain implementation enhances users' sense of security, this effect is significant primarily in contexts involving highly sensitive data. These findings suggest that the extent of blockchain adoption may be closely linked to information-sharing sensitivity [19]. Recognizing these advantages, an increasing number of enterprises are actively adopting blockchain and other financial technologies to strengthen information access channels and optimize decision-making processes. This adoption has triggered a positive chain reaction, gradually giving rise to a diffusion trend within the field of SCF. From a qualitative perspective, BCT can enhance the degree of information sharing among enterprises within a given scope. This increased transparency, in turn, attracts more enterprises to adopt blockchain, thereby promoting its continued diffusion.

Despite this positive feedback loop, several critical questions remain: Can empirical data confirm that improved information sharing directly increases the scale of blockchain adoption? Does greater information sharing accelerate the diffusion process? Is a higher degree of information sharing always beneficial for the diffusion of BCT? To address these issues, we incorporate the metric of information sharing sensitivity.

Information sharing sensitivity has emerged as a critical factor influencing blockchain adoption across supply chains, although its precise role remains debated in the literature. For example, Saberi et al. observed that in industries with stringent traceability requirements, such as pharmaceuticals, regulatory pressures heighten corporate sensitivity to information sharing, thereby promoting stronger blockchain adoption patterns [17]. Conversely, other studies highlight that oversensitivity to information protection can act as a barrier. Beck et al. found that enterprises frequently resist blockchain integration due to heightened concerns over protecting proprietary data, particularly in competitive markets where limited information sharing provides strategic advantages [20]. This resistance is further intensified in regulatory contexts, such as under GDPR, which adds complexity to enterprises' handling of sensitive cross-border data [21]. Consequently, scholarly opinion diverges on whether information-sharing sensitivity serves as a catalyst, by enhancing transparency, or as an inhibitor, through excessive protectionism.

To address the fundamental question: How exactly does information sharing sensitivity influence blockchain diffusion? We developed a rigorous mathematical framework to quantify its impact on adoption dynamics using systematic modeling and simulations.

The SEIR model, originally developed in epidemiology to study disease transmission dynamics, has increasingly been adapted to analyze technology diffusion due to its capacity of capturing social contagion effects and adoption thresholds. For example, Kiesling et al. extended the SEIR framework to investigate renewable energy technology adoption [22]. Their agent-based simulations demonstrated that policy interventions targeting early adopters could accelerate the transition from exposure to adoption. Further extensions of the SEIR model incorporate network heterogeneity and external interventions. For instance, Peres et al. introduced a threshold-modified SEIR model in marketing science, demonstrating how social network structures affect diffusion speed [23]. Juan Ding et al. developed an SEIR evolutionary game model that integrates game theory to investigate the spread and evolution of unsafe behaviors in chemical parks, overcoming the constraints of single-method modeling [24]. Their findings suggest that combining strict supervision by emergency management authorities with high-quality safety evaluations is more effective in controlling unsafe behavior diffusion. Despite its utility, SEIR-based models have been criticized for oversimplifying decision-making heterogeneity. Delre et al. recommended hybrid approaches that combine SEIR dynamics with discrete choice models to better capture individual-level adoption drivers [25]. Our model addresses this limitation by incorporating enterprise-type-dependent parameters. Moreover, conventional integer-order SEIR models cannot account for memory effects, where past behaviors continuously influence current adoption decisions. Fractional calculus, particularly the Caputo derivative, overcomes this limitation by introducing non-local operators with power-law memory kernels [26]. This feature reflects the persistent influence of past behaviors on diffusion. Zeng et al. investigated a fractional-order eco-epidemiological system with two delays, digestion and latency delays, incorporating pathogens as pest biocontrol agents [27]. Li et al. examined the role of time delay in a graded three species predator–prey model and a time graded reaction–diffusion system. Their work demonstrated the properties and stability of solutions in fractional order food chain models, showing that both types of systems undergo Hopf bifurcations as the delay parameter varies [28]. Therefore, we adopt the Caputo fractional derivative. The diffusion of BCT among enterprises can be effectively conceptualized as a contagion process, which is well captured by the SEIR framework. To more accurately represent the underlying dynamics, we adopt a fractional-order delayed SEIR

model. While SEIR extensions account for network effects [23] and policy interventions [22], they generally overlook the heterogeneous responsiveness of enterprises to information transparency. This oversight is particularly important in SCF contexts, where SMEs' adoption decisions are influenced by perceived risks associated with data sharing [20]. To address this, we introduce a nonlinear sensitivity index to quantify how enterprises' attitudes toward information sharing modulate blockchain diffusion dynamics.

The major contributions of this study are twofold. First, we develop a Caputo fractional-order SEIR model with time delays, which incorporates temporal intervals in the diffusion process and thereby aligns more closely with real-world adoption dynamics [29]. Second, we introduce a nonlinear index to quantify potential adopters' sensitivity to information sharing, where higher sensitivity corresponds to an increased willingness among enterprises to exchange data. Thus, in this study, we provide clear insights into the relationship between information sharing intensity and blockchain diffusion within supply chains, offering a foundation for designing effective strategies for technology implementation and adoption incentives.

The structure of this article is as follows: In Section 2, based on the SEIR model, we define four distinct states of enterprises in blockchain diffusion and their transition mechanisms; in Section 3 we formulate and analyze the SEIR mathematical model, examining the impact mechanisms of the nonlinear index. In Section 4, we present numerical simulations and their corresponding analyses. Finally, in Section 5 we conclude the study with a summary of key findings and identify the research limitations.

2. Description

The SEIR model simulates the spread of infectious diseases by describing the continuous flow of individuals among four distinct states: Susceptible (S), Exposed (E), Infectious (I), and Recovered (R). An outbreak typically originates from a small number of infectious individuals, who transmit the disease to susceptible individuals through contact at a certain probability. Upon infection, individuals do not immediately show symptoms; instead, they enter a latent period—the exposed state—during which they are not yet contagious. After an average incubation period, these exposed individuals transition to the infectious state, becoming capable of transmitting the disease and thereby driving the epidemic into a phase of rapid expansion. Concurrently, infectious individuals recover (or die) at a certain rate, exiting the transmission chain and moving into the recovered state, where they no longer participate in disease spread. The diffusion of BCT in SCF can be conceptualized as a dynamic, contagion-like process, closely resembling the transmission patterns observed in infectious disease epidemiology. Due to the core enterprises' strong capabilities and leading position in the industry, they are the first to engage with and adopt blockchain technology, acting as the initial adopters, serving as the primary sources of diffusion and entering an infectious state. Furthermore, SMEs that have not yet encountered the technology constitute the susceptible population. Through routine business interactions and transactional relationships with these infectious nodes, susceptible SMEs become exposed to BCT. This exposure initiates a critical evaluation period, analogous to the latent phase in disease models. During this period, spanning the interval from initial exposure to the final adoption decision, SMEs remain in an exposed state, actively assessing the technology's suitability, costs, and benefits. In this process, SMEs' willingness to adopt blockchain depends on their sensitivity to

information sharing. Within a certain threshold, increased sensitivity enhances enterprises' propensity to share information, thereby promoting more active adoption of BCT.

Upon successfully completing their evaluation, these SMEs formally adopt BCT, integrate it into their operations, and transition into an infectious state. In this capacity, they actively disseminate the technology through their own business networks, thereby accelerating its proliferation. Conversely, enterprises that exit the blockchain platform, whether due to contractual breaches, operational failures, or bankruptcy, enter a recovered state, analogous to the removed compartment in epidemiological models. Once in this recovered state, they no longer participate in the diffusion cycle, effectively terminating their role in propagating the technology.

This diffusion mechanism, interpreted through the lens of epidemic contagion, defines four distinct states:

(1) Susceptible State (S): SMEs that have not been exposed to BCT but have engaged in business transactions with enterprises that have adopted BCT. We classify these enterprises as non-adopting enterprises.

(2) Exposed State (E): SMEs that have been exposed to blockchain technology and are evaluating it to determine whether to adopt it, termed potential adopting enterprises.

(3) Infectious State (I): SMEs that have completed technology evaluation join the blockchain platform. We classify these enterprises as adopting enterprises.

(4) Recovered State (R): SMEs that exit the platform due to contract violations or bankruptcy, referred to as exiting enterprises.

3. Model and analysis

3.1. Model construction

Based on the preceding analysis, the four categories of enterprises in the diffusion process of BCT are: Non-adopting enterprises, potential adopters, adopting enterprises, and exiting enterprises. These correspond to the Susceptible (S), Exposed (E), Infectious (I), and Recovered (R) states, respectively, in an epidemiological contagion model. Within a certain range, higher sensitivity to information sharing strengthens potential adopters' willingness to exchange information, which in turn enhances their propensity to adopt BCT and promotes more comprehensive information sharing practices. As a result, the transition of enterprises from the non-adopting state to the adopting state increases. Conversely, lower sensitivity diminishes the willingness to share information and the likelihood of adoption, thereby reducing the flow from the Susceptible (S) to Infectious (I) states.

To capture this effect mathematically, we use a nonlinear incidence rate of the form $\beta S^p I$, where p denotes the information-sharing sensitivity, capturing nonlinear effects in information diffusion. The adoption of this form is based on the study by Liu et al., who employed an exponential expression when investigating infectious disease models with nonlinear incidence rates [30]. Furthermore, given that the sensitivity of information sharing fundamentally reflects the attitude and response intensity of S toward information, the exponential operation is applied to S.

Next, we explain the value and meaning of p:

- If $p = 1$, the model reduces to the classical linear propagation case, representing uniform information spread.

- If $p > 1$, a positive network feedback emerges: The greater the number of potential adopters, the stronger the information influence on each enterprise, thereby accelerating diffusion.
- If $p < 1$, an information damping effect occurs, where the diffusion speed decreases as the potential market expands.

To facilitate comprehension, a flowchart is presented to illustrate the diffusion process (see Figure 1).

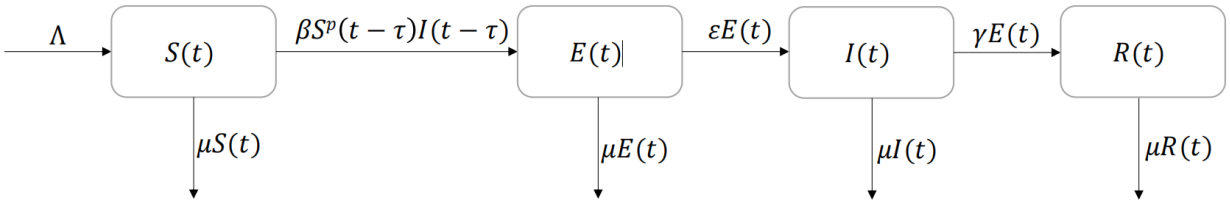

Figure 1. The diffusion process of BCT.

Figure 1 illustrates the dynamic diffusion process of BCT in SCF as a state-transition system. The process begins with new enterprises entering the Susceptible state, $S(t)$, at a constant rate Λ. The transition from the Susceptible state to the Exposed state, $E(t)$, denoting enterprises actively evaluating adoption. This is governed by the nonlinear term $\beta S^p(t-\tau)I(t-\tau)$, where β represents the diffusion efficiency between potential adopters and adopters, p captures potential adopters' sensitivity to information sharing, and τ denotes the duration between an enterprise's initial exposure to BCT and its final adoption decision, which we define as the evaluation period. This process encompasses a series of practical phases, including internal assessment, cost-benefit analysis, technical validation, and contract negotiation. Enterprises then progress from the exposed state $E(t)$ to the Infectious state $I(t)$, representing adopters that have fully integrated the technology into their operations, at a transition rate ε. Throughout this process, enterprises in all states (S, E, I) are subject to a constant bankruptcy or exit risk, μ, which transitions them to the Removed state $R(t)$.

In the context of SCF, the decision of enterprises to adopt BCT is fundamentally a form of financial behavior rooted in historical experience and risk memory. Enterprise decision-making does not rely solely on current market information but is deeply influenced by historical collaboration experiences, past financing outcomes, and accumulated judgments regarding the long-term credibility of the technology. This reflects the experience-weighted effect in financial behavior, where past events continuously influence current decisions in a gradually diminishing manner. Such dynamics are mathematically isomorphic to the power-law memory kernel of the Caputo fractional-order derivative.

The Caputo fractional derivative is defined as:

$$D_t^{\alpha} f(t) = \frac{1}{\Gamma(1-\alpha)} \int_0^t \frac{f'(\tau)}{(t-\tau)^{\alpha}} d\tau.$$

The fractional-order parameter α governs the decay rate of the memory kernel. As α approaches 1, the system behaves similarly to a classical memoryless differential system, reflecting the instantaneous

rate of state change with minimal influence from past behavior. This mathematical property corresponds to a high-frequency, real-time corporate decision-making pattern, in which firms closely monitor the latest market information and can rapidly adjust their financing strategies.

Conversely, as α approaches 0, the integral nature of the operator dominates. The system exhibits strong memory effects: The current state results from the cumulative integration of the historical trajectory, rather than merely reflecting instantaneous changes. In corporate financial behavior, this corresponds to a highly history-dependent, inertia-driven decision-making mode, where decisions regarding technology adoption, financing, and partnership formation are deeply rooted in long-established trust networks. This reflects a pattern characterized by robustness and prudence.

Based on this framework, we develop a Caputo fractional-order delayed SEIR model for SCF, which explicitly incorporates the impact of information-sharing sensitivity on BCT diffusion.

$$\begin{cases} D_t^\alpha S(t) = \Lambda - \beta S^p(t-\tau)I(t-\tau) - \mu S(t), & (1) \\ D_t^\alpha E(t) = \beta S^p(t-\tau)I(t-\tau) - (\mu+\varepsilon)E(t), & (2) \\ D_t^\alpha I(t) = \varepsilon E(t) - (\mu+\gamma)I(t), & (3) \\ D_t^\alpha R(t) = \gamma I(t) - \mu R(t). & (4) \end{cases} \tag{3.1}$$

All parameters are positive, reflecting their real-world interpretations in SCF. A disease-free equilibrium point $P_0(\frac{\Lambda}{\mu}, 0, 0, 0)$ always exists. The basic reproduction number $R_0 = \frac{\Lambda^p \beta \varepsilon}{\mu^p(\varepsilon+\mu)(\gamma+\mu)}$ is derived using the next-generation matrix method. By setting the four equations in (3.1) equal to zero, we obtain the endemic equilibrium point, $P^*(S^*, E^*, I^*, R^*)$, where

$$S^* = \frac{(\varepsilon+\mu)^{\frac{1}{p}}(\gamma+\mu)^{\frac{1}{p}}}{\beta^{\frac{1}{p}}\varepsilon^{\frac{1}{p}}}, \quad E^* = \frac{\gamma+\mu}{\varepsilon}I^*, \quad I^* = \frac{\Lambda\beta^{\frac{1}{p}}\varepsilon^{\frac{1}{p}} - \mu(\varepsilon+\mu)^{\frac{1}{p}}(\gamma+\mu)^{\frac{1}{p}}}{\beta^{\frac{1}{p}}\varepsilon^{\frac{1}{p}-1}(\varepsilon+\mu)(\gamma+\mu)}, \quad R^* = \frac{\gamma}{\mu}I^*.$$

Obviously, S^*, E^*, I^*, R^* must be positive. Therefore,

$$\Lambda\beta^{\frac{1}{p}}\varepsilon^{\frac{1}{p}} - \mu(\varepsilon+\mu)^{\frac{1}{p}}(\gamma+\mu)^{\frac{1}{p}} > 0,$$

thus,

$$\frac{\Lambda\beta^{\frac{1}{p}}\varepsilon^{\frac{1}{p}}}{\mu(\varepsilon+\mu)^{\frac{1}{p}}(\gamma+\mu)^{\frac{1}{p}}} > 1.$$

So

$$R_0 = \frac{\Lambda^p\beta\varepsilon}{\mu^p(\varepsilon+\mu)(\gamma+\mu)} = \left(\frac{\Lambda\beta^{\frac{1}{p}}\varepsilon^{\frac{1}{p}}}{\mu(\varepsilon+\mu)^{\frac{1}{p}}(\gamma+\mu)^{\frac{1}{p}}}\right)^p > 1.$$

Therefore, when $R_0 > 1$, the endemic equilibrium point exists.

To streamline the model analysis and highlight the core dynamic characteristics, we assume an information-sharing sensitivity index of $p = 1$, effectively representing a linear response of potential adopters to information sharing and modeling the technology contact rate in a bilinear form.

Then, we consider the coordinate transformation:

$$x(t) = S(t) - \bar{S}, \quad y(t) = E(t) - \bar{E}, \quad z(t) = I(t) - \bar{I}, \quad w(t) = R(t) - \bar{R},$$

where $\bar{S}$, $\bar{E}$, $\bar{I}$, and $\bar{R}$ represent the mean values of each respective state.

Linearizing system (3.1), we obtain:

$$\begin{cases} D_t^\alpha x(t) = -\beta\bar{I}x(t-\tau) - \beta\bar{S}z(t-\tau) - \mu x(t), \\ D_t^\alpha y(t) = \beta\bar{I}x(t-\tau) + \beta\bar{S}z(t-\tau) - (\varepsilon+\mu)y(t), \\ D_t^\alpha z(t) = \varepsilon y(t) - (\gamma+\mu)z(t), \\ D_t^\alpha w(t) = \gamma z(t) - \mu w(t). \end{cases}$$

Taking Laplace transforms on both sides, we obtain:

$$A(s)\cdot\begin{pmatrix} S(s) \\ E(s) \\ I(s) \\ R(s) \end{pmatrix} = \begin{pmatrix} a_1(s) \\ a_2(s) \\ a_3(s) \\ a_4(s) \end{pmatrix},$$

where,

$$\begin{aligned} a_1(s) &= s^{\alpha-1}x(0) - \beta\bar{I}e^{-s\tau}\int_{-\tau}^{0} e^{-st}\varphi_1(t)dt - \beta\bar{S}e^{-s\tau}\int_{-\tau}^{0} e^{-st}\varphi_2(t)dt, \\ a_2(s) &= s^{\alpha-1}y(0) + \beta\bar{I}e^{-s\tau}\int_{-\tau}^{0} e^{-st}\varphi_1(t)dt + \beta\bar{S}e^{-s\tau}\int_{-\tau}^{0} e^{-st}\varphi_2(t)dt, \\ a_3(s) &= s^{\alpha-1}z(0), \\ a_4(s) &= s^{\alpha-1}w(0). \end{aligned}$$

Subsequently, we arrive at the following expression for $A(s)$:

$$A(s) = \begin{pmatrix} s^\alpha + \beta\bar{I}e^{-s\tau} + \mu & 0 & \beta\bar{S}e^{-s\tau} & 0 \\ \beta\bar{I}e^{-s\tau} & s^\alpha + \varepsilon + \mu & \beta\bar{S}e^{-s\tau} & 0 \\ 0 & -\varepsilon & s^\alpha + \gamma + \mu & 0 \\ 0 & 0 & -\gamma & s^\alpha + \mu \end{pmatrix}. \tag{3.2}$$

3.2. The stability of the disease-free equilibrium point

Theorem 1. When $R_0 < 1$, $\tau \geq 0$, the disease-free equilibrium point $P_0(\frac{\Lambda}{\mu}, 0, 0, 0)$ is locally asymptotically stable.

Proof. Substitute $\bar{S}$ and $\bar{I}$ with $\frac{\Lambda}{\mu}$ and 0 into the matrix $A(s)$ (3.2). This yields the following result:

$$A(s) = \begin{pmatrix} s^\alpha + \mu & 0 & \beta\frac{\Lambda}{\mu}e^{-s\tau} & 0 \\ 0 & s^\alpha + \varepsilon + \mu & \beta\frac{\Lambda}{\mu}e^{-s\tau} & 0 \\ 0 & -\varepsilon & s^\alpha + \gamma + \mu & 0 \\ 0 & 0 & -\gamma & s^\alpha + \mu \end{pmatrix}.$$

Its characteristic equation is

$$(s^\alpha+\mu)^2\left[(s^\alpha+\varepsilon+\mu)(s^\alpha+\gamma+\mu) - \beta\varepsilon\frac{\Lambda}{\mu}e^{-s\tau}\right] = 0.$$

Case 1: When $\tau = 0$, the characteristic equation can be decomposed into two separate conditions:

$$(s^\alpha + \mu)^2 = 0 \quad \text{or} \quad (s^\alpha + \varepsilon + \mu)(s^\alpha + \gamma + \mu) - \beta\varepsilon\frac{\Lambda}{\mu} = 0.$$

Let $s^\alpha = \lambda$, and the solution to the equation $(\lambda + \mu)^2 = 0$ is

$$\lambda = -\mu < 0.$$

Consider the equation $(\lambda + \varepsilon + \mu)(\lambda + \gamma + \mu) - \beta\varepsilon\frac{\Lambda}{\mu} = 0$. This equation can be simplified, which yields

$$\lambda^2 + (\varepsilon + 2\mu + \gamma)\lambda + (\varepsilon + \mu)(\gamma + \mu) - \beta\varepsilon\frac{\Lambda}{\mu} = 0,$$

$$\lambda^2 + (\varepsilon + 2\mu + \gamma)\lambda + (\varepsilon + \mu)(\gamma + \mu)(1 - R_0) = 0.$$

When $R_0 < 1$, the characteristic roots satisfy $\lambda_1 + \lambda_2 < 0$ and $\lambda_1 \cdot \lambda_2 > 0$. According to Lyapunov's first method, all characteristic roots have negative real parts. Therefore, by the Routh–Hurwitz stability criterion, the disease-free equilibrium P_0 is locally asymptotically stable. Conversely, when $R_0 > 1$, at least one eigenvalue has a positive real part.

Case 2: When $\tau > 0$, consider the equation

$$s^{2\alpha} + (\varepsilon + 2\mu + \gamma)s^\alpha + (\varepsilon + \mu)(\gamma + \mu) - \beta\varepsilon\left(\frac{\Lambda}{\mu}\right)e^{-s\tau} = 0.$$

As a standard approach to determine the Hopf bifurcation threshold, we assume that the characteristic equation admits a purely imaginary solution.

$$s = i\omega = \omega e^{\frac{i\pi}{2}} \quad (\omega > 0)$$

be such a root; by substituting this into the characteristic equation, we obtain:

$$\omega^{2\alpha}(\cos\alpha\pi + i\sin\alpha\pi) + (\varepsilon + 2\mu + \gamma)\omega^\alpha\left(\cos\frac{\alpha\pi}{2} + i\sin\frac{\alpha\pi}{2}\right) + (\varepsilon + \mu)(\gamma + \mu) - \beta\varepsilon\left(\frac{\Lambda}{\mu}\right)(\cos\omega\tau - i\sin\omega\tau) = 0.$$

By separating the equation into its real and imaginary components and setting each to zero, we obtain the following results:

$$\begin{cases} \cos\omega\tau = \frac{D_1 + D_2 + C}{M}, \\ \sin\omega\tau = \frac{D_3 + D_4}{-M}, \end{cases} \tag{3.3}$$

where

$$\begin{aligned} D_1 &= \omega^{2\alpha}\cos\alpha\pi, \\ D_2 &= (\varepsilon + 2\mu + \gamma)\cos\frac{\alpha\pi}{2}\omega^\alpha, \\ D_3 &= \omega^{2\alpha}\sin\alpha\pi, \\ D_4 &= (\varepsilon + 2\mu + \gamma)\sin\frac{\alpha\pi}{2}\omega^\alpha, \end{aligned}$$

$$C = (\varepsilon + \mu)(\gamma + \mu),$$
$$M = \beta\varepsilon\frac{\Lambda}{\mu}.$$

According to $\cos^2(\omega\tau) + \sin^2(\omega\tau) = 1$, squaring both equations in (3.3) and summing them yields the following expression:

$$\omega^{4\alpha} + (\varepsilon + 2\mu + \gamma)^2\omega^{2\alpha} + 2D_1D_2(1 + C) + 2D_3D_4 + C^2 - M^2 = 0.$$

Let $z = \omega^{2\alpha}$ and $z > 0$, By substituting this into the above equation, we obtain

$$z^2 + (\varepsilon + 2\mu + \gamma)^2 z + K + C(C + M)(1 - R_0) = 0.$$

When $R_0 < 1$, this equation has no real solution. Therefore, the disease-free equilibrium point P_0 is locally asymptotically stable.

In summary, for $\tau \geq 0$, when $R_0 < 1$, the disease-free equilibrium P_0 remains locally asymptotically stable. $R_0 < 1$ means that a core enterprise that has adopted blockchain technology will successfully develop and convert fewer than one potential enterprise over the cycle. This indicates that the diffusion process cannot sustain itself and will diminish naturally.

3.3. The stability of the positive equilibrium point

Theorem 2. When $R_0 > 1$ and $T_1T_3 + T_2T_4 > 0$, there are

1) When $\tau \in [0, \tau_0]$, the system is locally asymptotically stable at the positive (endemic) equilibrium point.

2) When $\tau > \tau_0$, the system becomes unstable at the positive equilibrium. At $\tau = \tau_0$, the transversality condition is satisfied, and a Hopf bifurcation occurs in the vicinity of the equilibrium point.

Proof. The characteristic matrix of the system at the positive equilibrium point is:

$$A_2(s) = \begin{pmatrix} s^\alpha + \beta I^* e^{-s\tau} + \mu & 0 & \beta S^* e^{-s\tau} & 0 \\ \beta I^* e^{-s\tau} & s^\alpha + \varepsilon + \mu & \beta S^* e^{-s\tau} & 0 \\ 0 & -\varepsilon & s^\alpha + \gamma + \mu & 0 \\ 0 & 0 & -\gamma & s^\alpha + \mu \end{pmatrix}. \tag{3.4}$$

Let $b_1 = \beta I^*$, $b_2 = \mu$, $b_3 = \varepsilon + \mu$, $b_4 = \gamma + \mu$, $b_5 = \beta S^*$, and characteristic equation of (3.4) is:

$$s^{4\alpha} + \nu_1 s^{3\alpha} + \nu_2 s^{2\alpha} + \nu_3 s^\alpha + \nu_4 + (\nu_5 s^{3\alpha} + \nu_6 s^{2\alpha} + \nu_7 s^\alpha + \nu_8)e^{-s\tau} = 0, \tag{3.5}$$

where,

$$\nu_1 = 2b_2 + b_3 + b_4,$$
$$\nu_2 = b_2^2 + 2b_2b_3 + 2b_2b_4 + b_3b_4,$$
$$\nu_3 = 2b_2b_3b_4 + b_2^2b_3 + b_2^2b_4,$$
$$\nu_4 = b_2^2b_3b_4,$$

$$\nu_5 = b_1,$$

$$\nu_6 = b_1b_2 + b_1b_3 + b_1b_4 + \varepsilon b_5,$$

$$\nu_7 = b_1b_2b_3 + b_1b_2b_4 + b_1b_3b_4 + 2\varepsilon b_2b_5,$$

$$\nu_8 = b_1b_2b_3b_4 + \varepsilon b_2^2 b_5.$$

We next analyze the characteristic equation based on the value of τ.

Case 1: When $\tau = 0$,

Equation (3.5) reduces to

$$s^{4\alpha} + (\nu_1 + \nu_5)s^{3\alpha} + (\nu_2 + \nu_6)s^{2\alpha} + (\nu_3 + \nu_7)s^{\alpha} + \nu_4 + \nu_8 = 0.$$

According to the *Routh-Hurwitz* stability criterion, when the condition

$$\begin{cases} \nu_1 + \nu_5 > 0, \quad \nu_2 + \nu_6 > 0, \quad \nu_3 + \nu_7 > 0, \quad \nu_4 + \nu_8 > 0 \\ (\nu_1 + \nu_5)(\nu_2 + \nu_6)(\nu_3 + \nu_7) > (\nu_3 + \nu_7)^2 + (\nu_1 + \nu_5)^2(\nu_4 + \nu_8) \end{cases}$$

is satisfied.

All characteristic roots have negative real parts, indicating that the positive (endemic) equilibrium point is locally asymptotically stable.

Case 2: When $\tau > 0$, We consider the equation below

$$s^{4\alpha} + \nu_1 s^{3\alpha} + \nu_2 s^{2\alpha} + \nu_3 s^{\alpha} + \nu_4 + \left(\nu_5 s^{3\alpha} + \nu_6 s^{2\alpha} + \nu_7 s^{\alpha} + \nu_8\right) e^{-s\tau} = 0. \tag{3.6}$$

Suppose it has a pure virtual root $s = i\omega = \omega e^{\frac{\pi}{i}} (\omega > 0)$, by substituting, we obtain

$$(G_1 + iG_2) + (G_3 + iG_4)(\cos(\omega\tau) - i\sin(\omega\tau)) = 0,$$

where,

$$G_1 = \cos(2\alpha\pi)\omega^{4\alpha} + \nu_1 \cos\left(\frac{3}{2}\alpha\pi\right)\omega^{3\alpha} + \nu_2 \cos(\alpha\pi)\omega^{2\alpha} + \nu_3 \cos\left(\frac{\alpha}{2}\pi\right)\omega^{\alpha} + \nu_4,$$

$$G_2 = \sin(2\alpha\pi)\omega^{4\alpha} + \nu_1 \sin\left(\frac{3}{2}\alpha\pi\right)\omega^{3\alpha} + \nu_2 \sin(\alpha\pi)\omega^{2\alpha} + \nu_3 \sin\left(\frac{\alpha}{2}\pi\right)\omega^{\alpha},$$

$$G_3 = \nu_5 \cos\left(\frac{3}{2}\alpha\pi\right)\omega^{3\alpha} + \nu_6 \cos(\alpha\pi)\omega^{2\alpha} + \nu_7 \cos\left(\frac{\alpha}{2}\pi\right)\omega^{\alpha} + \nu_8,$$

$$G_4 = \nu_5 \sin\left(\frac{3}{2}\alpha\pi\right)\omega^{3\alpha} + \nu_6 \sin(\alpha\pi)\omega^{2\alpha} + \nu_7 \sin\left(\frac{\alpha}{2}\pi\right)\omega^{\alpha}.$$

By separating the equation into its real and imaginary components and setting each equal to zero, we obtain the following results:

$$\begin{cases} \cos(\omega\tau) = -\frac{G_1G_3 + G_2G_4}{G_3^2 + G_4^2}, \\ \sin(\omega\tau) = \frac{G_2G_3 - G_1G_4}{G_3^2 + G_4^2}. \end{cases} \tag{3.7}$$

Since $\cos^2(\omega\tau) + \sin^2(\omega\tau) = 1$, squaring both equations in (3.7) and summing them yields the following expression:

$$G_1^2 + G_2^2 = G_3^2 + G_4^2. \tag{3.8}$$

Rearranging Eq (3.8), we obtain

$$H(\omega) = \omega^{8\alpha} + \sum_{i=1}^{7} f_i(\nu_1, \nu_2, \nu_3, \cdots, \nu_8, \alpha)\omega^{i\alpha} + \mathcal{N} = 0.$$

Here, $f_i(\nu_1, \nu_2, \nu_3, \cdots, \nu_8, \alpha)$ serves as an abbreviation for the mathematical expression involving$\nu_1, \nu_2, \nu_3, \cdots, \nu_8$.

When $\mathcal{N} < 0$, since $H(0) < 0$, $\lim_{\omega\to+\infty} H(\omega) > 0$, and $H(\omega)$ is continuous, the Theorem of Existence of Zeroes guarantees at least one positive root. Consequently, the positive (endemic) equilibrium point is unstable.

Having established the possibility of instability, it is essential to characterize the nature of this transition. To confirm that a Hopf bifurcation occurs at $\tau = \tau_0$, we proceed to examine the transversality condition.

Let $s(\tau) = \xi(\tau) + i\omega(\tau)$, as the eigenvalue of Eq (3.6).

According to Eq (3.7), the bifurcation threshold expression is obtained:

$$\tau_j = \frac{1}{\omega_0}\left[\arccos\left(-\frac{G_1G_3 + G_2G_4}{G_3^2 + G_4^2}\right) + 2j\pi\right], \quad j = 0, 1, 2\ldots$$

We define a threshold value $\tau_0 = \min(\tau_j)$ such that $\xi(\tau_0) = 0$, $\omega(\tau_0) = \omega_0$.

The characteristic equation (3.6) is reduced to $Q_1(s) + Q_2(s)e^{-s\tau} = 0$, where,

$$Q_1(s) = s^{4\alpha} + \nu_1 s^{3\alpha} + \nu_2 s^{2\alpha} + \nu_3 s^{\alpha} + \nu_4,$$
$$Q_2(s) = \nu_5 s^{3\alpha} + \nu_6 s^{2\alpha} + \nu_7 s^{\alpha} + \nu_8.$$

Given the complexity of directly computing $\frac{ds}{d\tau}$, we instead determine $\left(\frac{ds}{d\tau}\right)^{-1}$ by applying the inverse function theorem.

$$\left(\frac{ds}{d\tau}\right)^{-1} = \frac{e^{s\tau}[Q_1'(s) + Q_2'(s)] - \tau}{sQ_2(s)} - \frac{\tau}{s}.$$

Then, we separate the real and imaginary parts:

$$\left(\frac{ds}{d\tau}\right)^{-1} = \frac{T_3 + iT_4}{T_1 + iT_2} - \frac{\tau_0}{i\omega_0},$$

where,

$$T_1 = -\omega_0 I_m[Q_2(i\omega_0)],$$

$$T_2 = \omega_0 \,\mathrm{Re}[Q_2(i\omega_0)],$$

$$T_3 = \mathrm{Re}[Q_1'(i\omega_0) + Q_2'(i\omega_0)]\cos(\omega_0\tau_0) - I_m[Q_1'(i\omega_0) + Q_2'(i\omega_0)]\sin(\omega_0\tau_0),$$

$$T_4 = I_m[Q_1'(i\omega_0) + Q_2'(i\omega_0)]\cos(\omega_0\tau_0) + \mathrm{Re}[Q_1'(i\omega_0) + Q_2'(i\omega_0)]\sin(\omega_0\tau_0).$$

Therefore,

$$\mathrm{Re}\left[\left(\frac{ds}{d\tau}\right)^{-1}\right]_{\tau=\tau_0} = \frac{T_1T_3 + T_2T_4}{T_1^2 + T_2^2}.$$

When $T_1T_3 + T_2T_4 > 0$, $\mathrm{Re}\left[\left(\frac{ds}{d\tau}\right)^{-1}\right]_{\tau=\tau_0} > 0$, thus $\frac{ds}{d\tau}\Big|_{\tau=\tau_0} > 0$, and the system satisfies the transversality condition for a Hopf bifurcation.

In summary, when $\tau \in [0, \tau_0]$ the positive equilibrium point is locally asymptotically stable. Given that $\tau \in [0, \tau_0]$, the evaluation cycle is relatively short, and the enterprise's technology assessment and decision-making processes proceed smoothly.

Information flows in a timely manner, and successful use cases can be observed and trusted relatively quickly by potential adopters. Market confidence in blockchain technology strengthens steadily as the number of adopters increases. Ultimately, the quantities in each state converge toward a steady equilibrium.

When $\tau > \tau_0$, the extended evaluation period destabilizes the equilibrium state of blockchain adoption dynamics and induces sustained periodic oscillations. The underlying real world mechanism is that an excessively long evaluation and decision making cycle introduces a significant time lag between market information and adoption behavior. Positive signals of rising adoption rates require a prolonged delay to stimulate new adoption decisions. By the time firms adopt, market conditions may have shifted, and previously accumulated issues (such as implementation difficulties or lower than expected returns) begin to surface, generating negative feedback. These negative signals, in turn, take time to propagate and affect subsequent decisions, leading to a decline in adoption rates. This cycle repeats, resulting in periodic fluctuations in market adoption driven endogenously by decision making delays.

In summary, τ_0 represents the critical threshold at which the system transitions from a stable diffusion state to a state of periodic oscillations. This indicates the maximum delay induced by the evaluation of BCT that the system can tolerate while maintaining a steady-state diffusion. A higher value of τ_0 suggests a greater industry tolerance for prolonged evaluation processes, implying that the promotion of BCT is less susceptible to destabilization caused by evaluation delays.

3.4. The effect of α on τ_0

To express the relationship between α and τ_0 more explicitly, we rewrite Eq (3.8) as:

$$G_1(\omega, \alpha)^2 + G_2(\omega, \alpha)^2 = G_3(\omega, \alpha)^2 + G_4(\omega, \alpha)^2.$$

It is not difficult to see that ω is an implicit function of α. Therefore, applying the chain rule and differentiating both sides with respect to α, we obtain:

$$2G_1\frac{\partial G_1}{\partial \omega}\frac{d\omega}{d\alpha} + 2G_1\frac{\partial G_1}{\partial \alpha} + 2G_2\frac{\partial G_2}{\partial \omega}\frac{d\omega}{d\alpha} + 2G_2\frac{\partial G_2}{\partial \alpha} = 2G_3\frac{\partial G_3}{\partial \omega}\frac{d\omega}{d\alpha} + 2G_3\frac{\partial G_3}{\partial \alpha} + 2G_4\frac{\partial G_4}{\partial \omega}\frac{d\omega}{d\alpha} + 2G_4\frac{\partial G_4}{\partial \alpha}.$$

After simplification, we obtain:

$$\frac{d\omega}{d\alpha} = -\frac{G_1\frac{\partial G_1}{\partial \alpha} + G_2\frac{\partial G_2}{\partial \alpha} - G_3\frac{\partial G_3}{\partial \alpha} - G_4\frac{\partial G_4}{\partial \alpha}}{G_1\frac{\partial G_1}{\partial \omega} + G_2\frac{\partial G_2}{\partial \omega} - G_3\frac{\partial G_3}{\partial \omega} - G_4\frac{\partial G_4}{\partial \omega}}.$$

According to Eq (3.9), we obtain:

$$\tau_0 = \frac{1}{\omega_0}\arccos\left(-\frac{G_1G_3 + G_2G_4}{G_3^2 + G_4^2}\right). \tag{3.10}$$

Let $-\frac{G_1G_3 + G_2G_4}{G_3^2 + G_4^2} = U$, and then take the derivative of both sides with respect to α.
Therefore, we have:

$$\frac{d\tau_0}{d\alpha} = \frac{-\frac{1}{\sqrt{1-U^2}}\frac{\partial U}{\partial \alpha}\omega_0 - \frac{d\omega_0}{d\alpha}\arccos U}{\omega_0^2}. \tag{3.11}$$

Although we have derived the expression for $\frac{d\tau_0}{d\alpha}$, due to the complex coupling terms involving fractional-order exponential functions and trigonometric functions, its sign cannot be uniformly determined through purely analytical means. Essentially, the positivity or negativity depends on the values of the system parameters and the interval in which α lies, reflecting the complexity of nonlinear coupling in fractional-order time-delay systems. In subsequent chapters, we will employ numerical simulations to compute and analyze this derivative under different parameter combinations, thereby revealing the relationship between τ_0 and α.

3.5. The impact of p on the diffusion process

Theorem 3.

1) When $\left[1 - \frac{\beta S_0^p \tau\varepsilon}{\mu+\varepsilon} + 2\tau(\gamma+\mu)\right] > 0$, the diffusion speed of BCT increases monotonically with the parameter p.

2) When $\left[1 - \frac{\beta S_0^p \tau\varepsilon}{\mu+\varepsilon} + 2\tau(\gamma+\mu)\right] < 0$, the diffusion speed of BCT decreases monotonically with the parameter p.

Proof. The diffusion speed of reaction-diffusion models is a central research focus, and Thieme and Zhao demonstrated that this speed coincides with the minimal wave speed of traveling waves [31]. In SCF, enterprises are not uniformly distributed but instead form spatial structures along supply chain networks or geographic regions. The diffusion of BCT typically propagates spatially through transaction links or industry clusters. Therefore, we introduce the spatial variable $x \subseteq \mathbb{R}^n$. The adoption behavior of BCT spreads in space through inter-enterprise interactions such as contact and transactions, a process that can be modeled as diffusion. Furthermore, since E and I represent active states in technology propagation, diffusion is assumed to act only on E and I. Thus, by incorporating Laplace operator terms $D_E\nabla^2 E$ and $D_I\nabla^2 I$ into the Eqs (3.1) (2) and (3), respectively, they represent the spatial influence of E and I on neighboring enterprises. Therefore, we obtain the following fractional-order delayed reaction–diffusion system:

$$\begin{cases} D_t^\alpha E(x,t) = D_E \nabla^2 E + \beta S^p(t-\tau,x) I(t-\tau,x) - (\mu+\varepsilon)E(x,t), \quad (1) \\ D_t^\alpha I(x,t) = D_I \nabla^2 I + \varepsilon E(x,t) - (\mu+\gamma) I(x,t). \quad (2) \end{cases} \tag{3.12}$$

D_E and D_I are diffusion coefficients, reflecting the spatial efficiency of propagation.

To analyze the propagation speed of BCT in SCF, we assume that the diffusion process occurs along the dominant direction of propagation, which corresponds to the primary pathway of BCT diffusion within the SCF (e.g., vertical transmission from a core enterprise to multi-tier suppliers). Under this assumption, we define the spatial coordinate x as the position along the propagation direction and seek traveling wave solutions of the form

$$E(x,t) = E(z), \quad I(x,t) = I(z), \quad z = x - ct, \tag{3.13}$$

where c represents the wave speed.

Based on the properties of the time-fractional derivative under traveling wave transformation [32], we have:

$$D_t^\alpha I(x,t) = (-c)^\alpha \frac{d^\alpha I}{dz^\alpha}.$$

Then, by substituting expression (3.14) into Eqs (3.12) and (3.13), we arrive at

$$(-c)^\alpha \frac{d^\alpha I}{dz^\alpha} = D_I \frac{d^2 I}{dz^2} + \varepsilon E - (\gamma+\mu) I. \tag{3.14}$$

Assuming the traveling wave solution is approximately determining the diffusion speed of BCT along the supply chain network, it mathematically corresponds to solving for the wave speed c of the system's traveling wave solution. However, a traveling wave spatially connects two equilibrium states, the diffused state behind the wavefront and the undiffused state ahead, and its speed is not arbitrary but uniquely determined by the system parameters. This determinacy stems from the linear stability analysis of the wavefront: A traveling wave solution exists and remains stable only if the wave speed c ensures monotonic exponential decay of the wavefront to zero in the undiffused region [33]. Therefore, we first linearize the system in the wavefront region where $I, E \approx 0$, and we assume the wavefront solution takes the form of an exponential decay [33]:

$$I(z) \sim e^{-\vartheta z}, \quad \vartheta > 0.$$

In his seminal work, Podlubny points out that fractional derivatives correspond to the multiplier $(iw)^\alpha$ in the Fourier transform domain [34]. Accordingly, in the traveling wave analysis, we can assume:

$$\frac{d^\alpha}{dz^\alpha} e^{-\vartheta z} = (-\vartheta)^\alpha e^{-\vartheta z}.$$

Substituting it into (3.14), we obtain:

$$(c\vartheta)^\alpha e^{-\vartheta z} = D_I \vartheta^2 e^{-\vartheta z} + \varepsilon E(z) - (\gamma+\mu) I. \tag{3.15}$$

In the wavefront region, enterprises ahead have not been influenced by the diffusion of BCT, and, thus, the density of susceptible enterprises S remains approximately at its initial value S_0. Moreover,

since the density of exposed enterprises E in this region is extremely low, its spatial gradients can be neglected. As a result, the diffusion term $D_E\nabla^2 E$ can be omitted. Additionally, similarly to I, E also satisfies the following equation:

$$E(z) \sim e^{-\vartheta z}, \quad \vartheta > 0.$$

Based on this, Eq (3.12) can be simplified to:

$$(c\vartheta)^\alpha E(z) = \beta S_0^p I(z + c\tau) - (\mu + \varepsilon)E(z) = \beta S_0^p e^{-\vartheta c\tau} I(z) - (\mu + \varepsilon)E(z).$$

Thus,

$$E(z) = \frac{\beta S_0^p e^{-\vartheta c\tau}}{(c\vartheta)^\alpha + \mu + \varepsilon} I(z).$$

In this section, we focus on the early stage of BCT diffusion, specifically the wavefront of the traveling wave solution. In this region, where the technology has just begun to penetrate, the propagation speed approaches its theoretical minimum, making the contribution of the wave propagation term $(c\vartheta)^\alpha$ negligible. Consequently, the internal transition rate $\mu + \varepsilon$ becomes dominant. Therefore, the wavefront satisfies the following condition:

$$(c\vartheta)^\alpha \ll \mu + \varepsilon.$$

Therefore,

$$E(z) \approx \frac{\beta S_0^p e^{-\vartheta c\tau}}{\mu + \varepsilon} I(z). \tag{3.16}$$

We substitute expression (3.16) into Eq (3.15) to obtain:

$$(c\vartheta)^\alpha = D_I\vartheta^2 + \varepsilon\frac{\beta S_0^p e^{-\vartheta c\tau}}{\mu + \varepsilon} - (\gamma + \mu). \tag{3.17}$$

Given that the analysis is conducted in the wavefront region, the product $\vartheta c\tau$ is small. Additionally, in this section, we focus exclusively on the case of weak memory effects (α approaching 1). Scenarios with more pronounced memory effects will be examined in future work. Therefore, the following two expressions hold:

$$e^{-\vartheta c\tau} \approx 1 - \vartheta c\tau, \quad (c\vartheta)^\alpha \approx c\vartheta.$$

Substituting this approximation into Eq (3.17) and simplifying yields the following quadratic form:

$$D_I\vartheta^2 + \left(-c - \frac{\beta S_0^p c\tau\varepsilon}{\mu + \varepsilon}\right)\vartheta + \frac{\beta S_0^p \varepsilon}{\mu + \varepsilon} - (\gamma + \mu) = 0. \tag{3.18}$$

The minimum wave speed is determined by setting the discriminant of Eq (3.18) to zero, thereby ensuring the existence of a critical traveling wave solution. This gives:

$$C_{\min} = \frac{2\sqrt{D_I\left(\frac{\beta S_0^p \varepsilon}{\mu+\varepsilon} - \gamma - \mu\right)}}{1 + \frac{\beta S_0^p \tau \varepsilon}{\mu+\varepsilon}}.$$

Here, $\frac{\beta S_0^p \varepsilon}{\mu+\varepsilon} - \gamma - \mu \geq 0$ must hold. Otherwise, the minimal wave speed does not exist.

We then proceed to take the derivative with respect to p, obtaining

$$\frac{dC_{\min}}{dp} = \frac{\beta S_0^p \varepsilon \ln S_0 \sqrt{D_I}}{(\mu+\varepsilon)\left(1 + \frac{\beta S_0^p \tau \varepsilon}{\mu+\varepsilon}\right)^2 \sqrt{\frac{\beta S_0^p \varepsilon}{\mu+\epsilon} - \gamma - \mu}} \cdot \left[1 - \frac{\beta S_0^p \tau \varepsilon}{\mu+\varepsilon} + 2\tau(\gamma+\mu)\right].$$

Since S represents the initial number of enterprises, its value is greater than or equal to 1 and $\ln S_0 \geq 0$.

Thus, when

$$\left[1 - \frac{\beta S_0^p \tau \varepsilon}{\mu+\varepsilon} + 2\tau(\gamma+\mu)\right] > 0, \quad \frac{dC_{\min}}{dp} > 0, \quad C_{\min} \text{ increases with the increase of } p.$$

However, when

$$\left[1 - \frac{\beta S_0^p \tau \varepsilon}{\mu+\varepsilon} + 2\tau(\gamma+\mu)\right] < 0, \quad \frac{dC_{\min}}{dp} < 0, \quad C_{\min} \text{ decreases with the increase of } p.$$

Since the minimal wave speed corresponds to the actual propagation speed [35], $C_{\min}$ represents the diffusion speed of BCT.

This suggests that a higher degree of information sharing does not necessarily facilitate faster diffusion of BCT.

Examining expression $\left[1 - \frac{\beta S_0^p \tau \varepsilon}{\mu+\varepsilon} + 2\tau(\gamma+\mu)\right]$ while keeping other parameters fixed, an increase in p may cause the value of the expression to become negative. In this case, $C_{\min}$ and p exhibit a negative correlation. In the context of SCF, this corresponds to a scenario in which higher sensitivity of enterprises to information accelerates the spread of BCT around core enterprises, leading to the rapid formation of dense clusters of adoption among nearby suppliers. However, this concentration of information within central regions results in informational saturation, which undermines the driving force for frontier propagation. Consequently, the overall diffusion speed is reduced.

Theorem 4. When

$$\left|\frac{\beta S_0^p \varepsilon}{\mu+\varepsilon} - \gamma - \mu\right| < 1, \ \alpha > 0,$$

the final adoption scale $\mathcal{F}$ increases monotonically with parameter p.

Proof. Given that the total number of enterprises is N, it follows from the original system (3.1) that:

$$D_t^\alpha N(t) = D_t^\alpha S(t) + D_t^\alpha E(t) + D_t^\alpha I(t) + D_t^\alpha R(t) = \Lambda - \mu N(t).$$

According to the study by Teng et al., the enterprise bankruptcy rate μ is 0.048 [2]. Therefore, we omit the term $\mu N(t)$ in the equation. This step constitutes a modeling approximation intended

to simplify the analysis and focus on the primary impact mechanism of the information sensitivity parameter p. This leads to:

$$D_t^\alpha N(t) = \Lambda.$$

Moreover, performing the inverse operation of Caputo fractional-order integration on both sides, we obtain:

$$N(t) = \frac{\Lambda}{\Gamma(\alpha)} \int_0^t (t-\tau)^{\alpha-1} d\tau + N(0) = \frac{\Lambda}{\Gamma(\alpha+1)} t^\alpha.$$

At the initial stage of diffusion, with $D_t^\alpha E(t) \approx 0$ and $S_0 \approx N$, substituting into Eq (3.1)(2) yields:

$$E(t) = \frac{\beta S_0^{\,p}}{\mu+\varepsilon} I. \tag{3.19}$$

Substituting this into the Eq (3.1)(3), and then taking the Laplace transform on both sides,

$$D_t^\alpha I(t) = \left(\frac{\beta S_0^{\,p} \varepsilon}{\mu+\varepsilon} - \gamma - \mu \right) I,$$

$$\mathcal{L}[D_t^\alpha I(t)] = s^\alpha \mathcal{L}[I(t)] - s^{\alpha-1} I_0 = k\mathcal{L}[I(t)],$$

$$\mathcal{L}[I(t)] = \frac{s^{\alpha-1} I_0}{s^\alpha - k},$$

where,

$$k = \frac{\beta S_0^{\,p} \varepsilon}{\mu+\varepsilon} - \gamma - \mu.$$

It is known that the Laplace transform of the Mittag-Leffler function is given by:

$$\mathcal{L}[E_\alpha(kt^\alpha)] = \frac{s^{\alpha-1}}{s^\alpha - k}.$$

Applying the inverse Laplace transform to $\mathcal{L}[I(t)] = \frac{s^{\alpha-1} I_0}{s^\alpha - k}$ yields the solution in the form:

$$I(t) = I_0 E_\alpha(kt^\alpha), \tag{3.20}$$

where

$$E_\alpha(z) = \sum_{n=0}^{\infty} \frac{z^n}{\Gamma(\alpha n + 1)}.$$

To examine how variations in p influence the adoption scale at fixed time points, independent of time t, we introduce a multiplier e^{-t} on the right-hand side of Eq (3.20). This yields $I_2(t)$ which exhibits the same monotonic behavior with respect to p as $I(t)$.

$$I_2(t) = I_0 e^{-t} E_\alpha(kt^\alpha). \tag{3.21}$$

As shown in Table 1, $\mathcal{F}$ represents the final adoption scale of BCT (the number of enterprises in state I when the system reaches a steady state).

Furthermore, we define a new variable $\mathcal{F}_2$ whose partial derivative with respect to p has the same sign as that of $\mathcal{F}$. Therefore, as p varies, $\mathcal{F}_2$ and $\mathcal{F}$ exhibit the same trend. The final adoption scale is obtained by integrating $I(t)$ with respect to time. According to the proof by Haubold et al. [36], we have

$$\int_0^{+\infty} e^{-t} E_\alpha(kt^\alpha)dt = \frac{1}{1-k}.$$

Thus,

$$\mathcal{F}_2 = \int_0^{+\infty} I_2(t)dt = \int_0^{+\infty} I_0 e^{-t} E_\alpha(kt^\alpha)dt = I_0 \frac{1}{1-k} = \frac{I_0}{1 - \frac{\beta S_0^p \varepsilon}{\mu+\varepsilon} + \gamma + \mu}. \tag{3.22}$$

When $|k| < 1, \alpha > 0$, the integral in (3.22) is well-defined [36]. We then differentiate it with respect to p.

$$\frac{\partial \mathcal{F}_2}{\partial p} = I_0 \frac{\beta S_0^p \varepsilon \ln S_0}{(1 - \frac{\beta S_0^p \varepsilon}{\mu+\varepsilon} + \gamma + \mu)^2} > 0.$$

Thus,

$$\frac{\partial \mathcal{F}}{\partial p} > 0.$$

In conclusion, as p increases, $\mathcal{F}$ also increases, resulting in a larger final adoption scale. As p increases, the willingness of enterprises to share information strengthens, leading to higher efficiency in information transmission. Consequently, adoption-related information from enterprises that have already adopted BCT is transmitted more quickly and extensively to those yet to adopt. This dynamic reduces perceived risks associated with BCT among enterprises and encourages them to follow the adoption trend. As a result, the overall adoption scale expands.

4. Numerical simulations

4.1. Numerical simulation of the disease-free equilibrium

Let the initial conditions be specified as

$$\alpha = 0.98, \quad p = 1, \quad \Lambda = 0.085, \quad \beta = 0.15, \quad \varepsilon = 0.1, \quad \mu = 0.048, \textit{and} \quad \gamma = 0.2$$

(see [2]).

The fractional order $\alpha = 0.98$ captures weak memory effects in enterprise decision-making, while the sensitivity index $p = 1$ represents the baseline linear scenario. This is then calculated to have $R_0 = 0.733 < 1$, $P_0(1.771, 0, 0, 0)$.

Without loss of generality, we select $\tau = 0.25$ year and $\tau = 2$ year to verify that the disease-free equilibrium point is locally asymptotically stable. This indicates that variations in the time delay do not affect the stability of the disease-free equilibrium.

Subsequently, we set the initial values of the SEIR to $(10, 0, 2, 0)$, which aligns with the realistic conditions of the early diffusion stage.

We performed numerical simulations using MATLAB and obtained the following results:

In Figures 2 and 3, the horizontal axis represents time in years, and the vertical axis represents the number of enterprises in units of individual firms. In the following analysis, the time variable t consistently denotes values measured in years. As can be observed from both figures, after undergoing dynamic changes, the number of enterprises converges to P_0, which corroborates our Theorem 1.

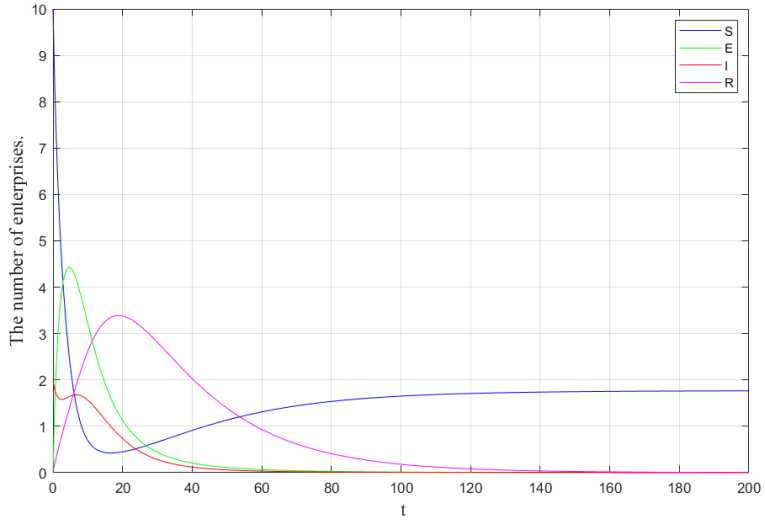

Figure 2. Stable phase diagram of a system with $\tau = 0.25$ when $R_0 < 1$.

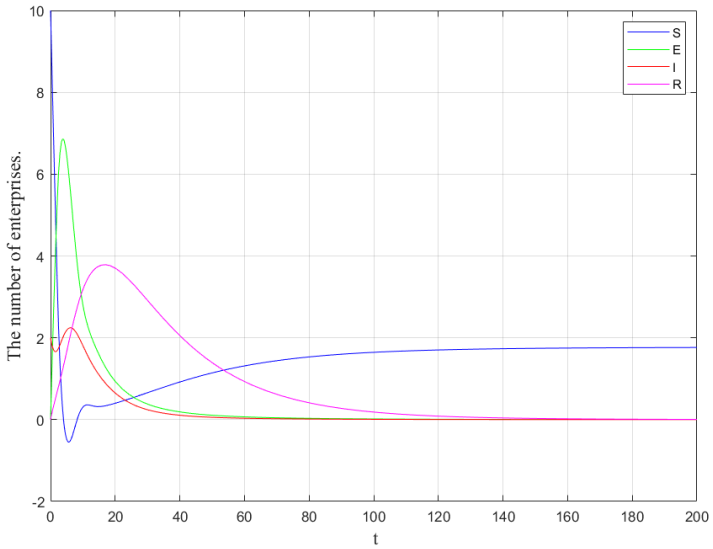

Figure 3. Stable phase diagram of a system with $\tau = 2$ when $R_0 < 1$.

Next, we examine the stability of S, E, I, and R under different initial conditions. Four sets of initial values are considered: $(10, 5, 1, 0)$, $(8, 18, 9, 2)$, $(12, 4, 18, 3)$, $(15, 23, 13, 8)$. This selection is guided by two principles: First, to ensure the initial states are realistic, with non-adopting enterprises comprising the majority while including potential adopters, adopters, and exited enterprises, thereby simulating plausible market scenarios; second, to demonstrate that the model's long-term dynamics and final equilibrium are determined primarily by system parameters rather than initial conditions, thereby reinforcing the universality and robustness of our conclusions.

As shown in Figure 4, differences in the initial values of S, E, I, and R do not alter the corresponding equilibrium outcomes. This demonstrates that when $R_0 < 1$, the value of I will converge to zero, and BCT fails to diffuse, regardless of the time delay τ.

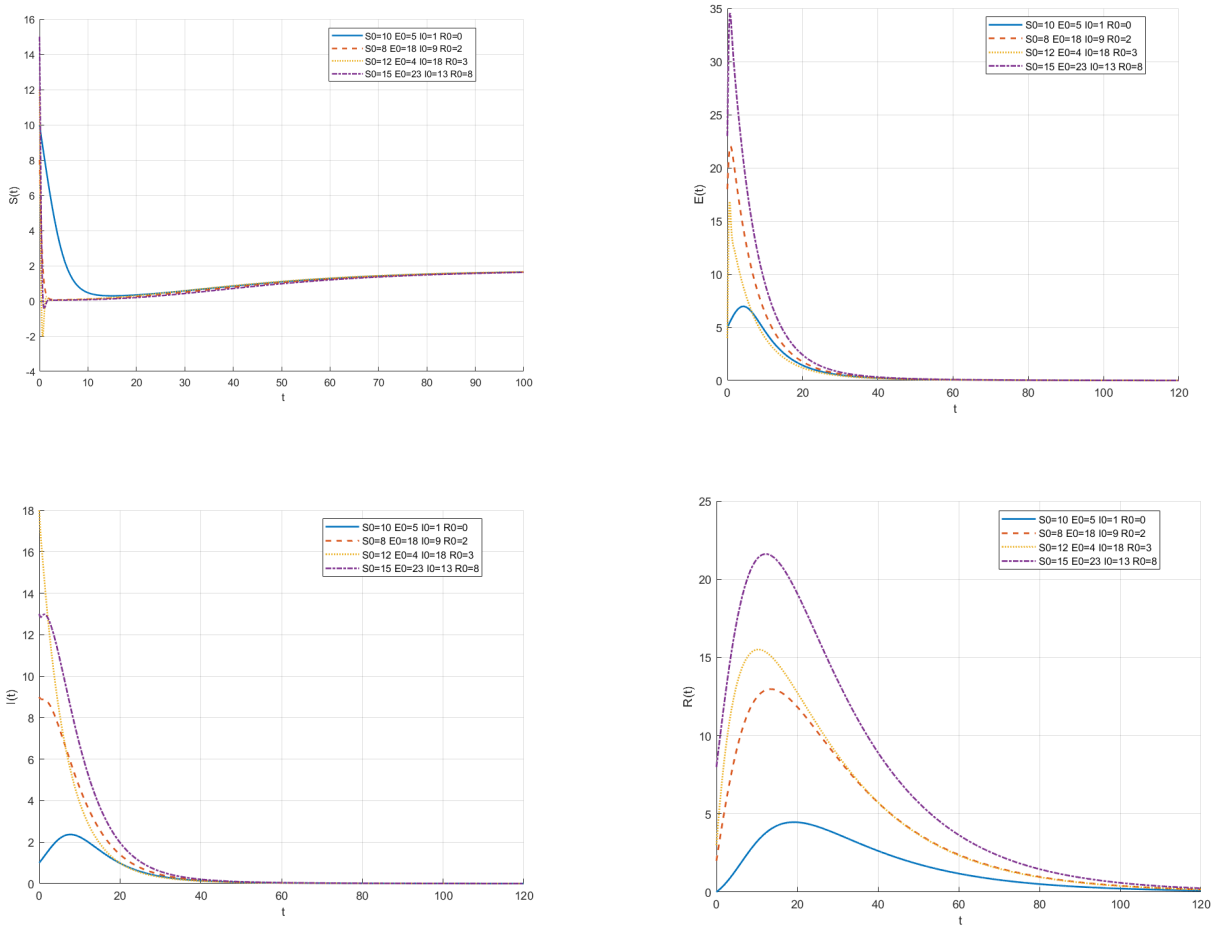

Figure 4. When $R_0 < 1$, it gives the change curve of S, E, I, R.

4.2. Numerical simulation of the positive equilibrium point

Let the initial conditions be specified as

$$\alpha = 0.98, \quad \Lambda = 0.085, \quad \beta = 0.25, \quad \mu = 0.048, \quad \varepsilon = 0.3, \quad \gamma = 0.1, \textit{and} \quad p = 1$$

(see [2]).

We then proceed to calculate the state variables to obtain.

$$R_0 = 2.579 > 1, \quad S^* = 0.687, \quad E^* = 0.15, \quad I^* = 0.303, \quad R^* = 0.631, \quad P^* = (0.687, 0.15, 0.303, 0.631).$$

Looking back to Section 3.4, it is important to emphasize that all our conclusions are derived from Eq (3.8). Since G_1, G_2, G_3, and G_4 are all functions of ω and α, Eq (3.8) can essentially be regarded as an equation $F(\omega, \alpha) = 0$. This implies that for a given value of α, ω is uniquely determined accordingly, establishing an implicit functional relationship between the two. Based on this, we employ the fzero algorithm to solve for the value of ω_0 corresponding to a specified α. Thus, this is calculated to have $\omega_0 = 0.164, \tau_0 = 12.011$.

Additionally, two distinct time delays, $\tau = 1$ and $\tau = 21.1$, are selected to accentuate contrasts in system behavior, providing a visual distinction between stable and oscillatory regimes.

i. When $\tau = 2 < \tau_0 = 12.011$, it is verified that the endemic equilibrium point is stable.

We then consider four sets of initial values, (1,0.5,1,0), (8,1.8,0.9,0.2), (1.2,0.4,0.18,0.3), (1.5,0.23,0.13,0.8) to examine the stability of the positive equilibrium under diverse initial conditions.

Figures 5 and 6 illustrate that when $R_0 > 1$ and $\tau < \tau_0$, the system's positive (endemic) equilibrium asymptotically converges to a stable state. This confirms that, under such parameter settings, BCT can be effectively adopted and sustained within SCF, reaching a steady diffusion state.

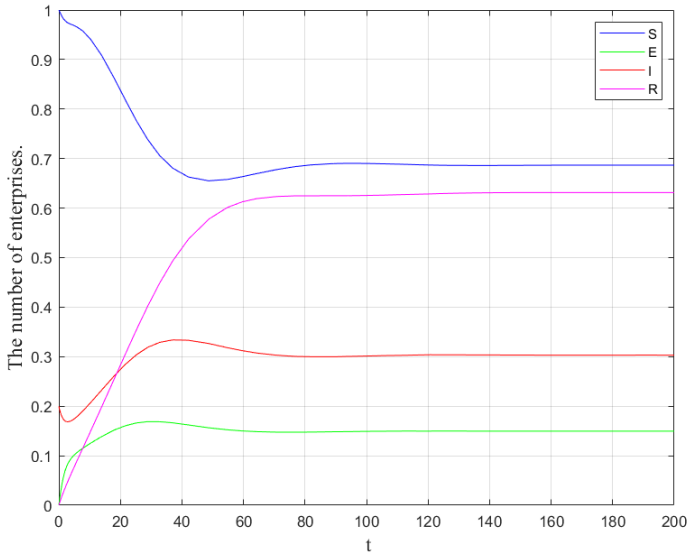

Figure 5. Stable phase diagram of a system with $\tau = 2 < \tau_0$ when $R_0 > 1$.

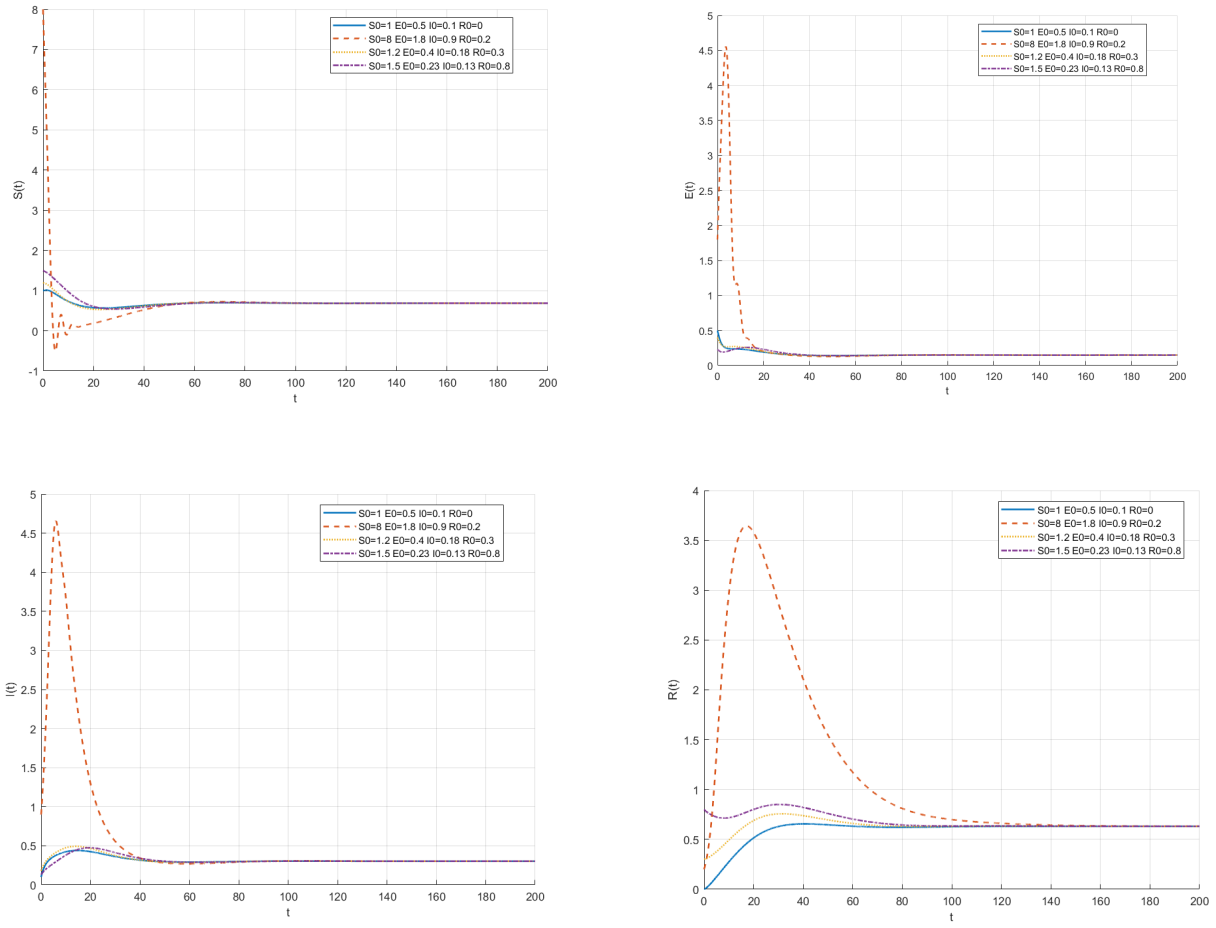

Figure 6. When $R_0 > 1$ with $\tau = 2 < \tau_0$, it gives the change curve of S, E, I, R.

ii. When $\tau = 21.1 > \tau_0$, the positive equilibrium point is unstable and a Hopf bifurcation occurs at P^*.

As shown in Figure 7, it depicts the system's dynamic behavior when the time delay exceeds its critical value. The positive equilibrium point P^* loses stability, triggering a Hopf bifurcation and the emergence of stable periodic oscillations. This indicates that enterprise technology adoption exhibits continuous, cyclical fluctuations rather than converging to a steady state. The research by Badakhshan et al. demonstrates that the bullwhip effect, a form of cyclical fluctuation in fund flows at the operational level, can be effectively prevented through blockchain-enabled data sharing [37]. This periodic fluctuation inherent in the bullwhip effect closely mirrors the oscillatory behavior explored in our own findings, thereby providing empirical support for our theoretical model. For the corresponding scenario in the context of SCF, please refer to the end of Section 3.3.

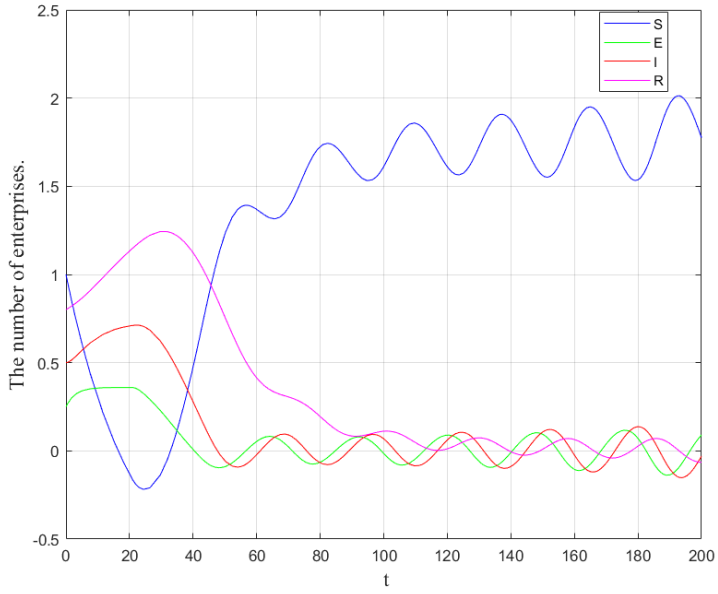

Figure 7. Phase diagram of the system when $\tau > \tau_0$.

4.3. The effect of p on the diffusion process

Analysis indicates that the minimum diffusion rate $C_{\min}$ may initially increase and then decrease with rising p under certain conditions, suggesting inherent trade-offs: Excessive information sharing sensitivity can undermine diffusion effectiveness. To verify this theorem, we select four distinct parameter sets exhibiting significant variation. These sets simulate diverse market environments and technological conditions while ensuring that the system remains within the diffusion regime. The objective is to demonstrate that, across these varying parameter environments, $C_{\min}$ consistently displays a non-monotonic pattern. The four sets of initial values are:

- **Group 1**: ($\beta = 0.001$, $S_0 = 50$, $\varepsilon = 0.2$, $\mu = 0.01$, $\gamma = 0.05$, $D_I = 0.1$, $\alpha = 0.8$, $\tau = 0.1$)
- **Group 2**: ($\beta = 0.002$, $S_0 = 30$, $\varepsilon = 0.3$, $\mu = 0.02$, $\gamma = 0.1$, $D_I = 0.2$, $\alpha = 0.82$, $\tau = 0.2$)
- **Group 3**: ($\beta = 0.0005$, $S_0 = 40$, $\varepsilon = 0.1$, $\mu = 0.005$, $\gamma = 0.02$, $D_I = 0.05$, $\alpha = 0.88$, $\tau = 0.15$)
- **Group 4**: ($\beta = 0.003$, $S_0 = 20$, $\varepsilon = 0.4$, $\mu = 0.015$, $\gamma = 0.08$, $D_I = 0.15$, $\alpha = 0.9$, $\tau = 0.25$)

In this model, $C_{\min}$ is a dimensionless velocity. As shown in Figure 8, all four datasets display a consistent unimodal trend, initially rising and then declining. This pattern highlights a nonlinear relationship, indicating that excessively high values of the information sharing sensitivity index p can paradoxically diminish the diffusion efficiency of BCT. For the corresponding scenario in the context of SCF, please refer to the end of Theorem 3, Section 3.5.

Next, we investigate whether the final adoption scale $\mathcal{F}$ increases. Four sets of initial values are selected to examine the sensitivity of the adoption scale to key parameters, including the transmission rate (β), the initial number of non-adopting enterprises (S_0), and the bankruptcy rate (μ). By varying these parameters while keeping all others constant, the analysis assesses whether technology adoption can expand under challenging conditions, such as low diffusion efficiency, high exit rates, or a limited initial market size.

- **Group 1**: ($\beta = 0.001$, $S_0 = 10$, $\varepsilon = 0.2$, $\mu = 0.01$, $\gamma = 0.05$, $I_0 = 100$)
- **Group 2**: ($\beta = 0.002$, $S_0 = 8$, $\varepsilon = 0.2$, $\mu = 0.01$, $\gamma = 0.1$, $I_0 = 100$)
- **Group 3**: ($\beta = 0.005$, $S_0 = 3$, $\varepsilon = 0.2$, $\mu = 0.01$, $\gamma = 0.1$, $I_0 = 100$)
- **Group 4**: ($\beta = 0.0005$, $S_0 = 20$, $\varepsilon = 0.2$, $\mu = 0.01$, $\gamma = 0.05$, $I_0 = 100$)

As shown in Figure 9, as p increases, the adoption scale $\mathcal{F}$ rises, meaning more enterprises join the blockchain. For the corresponding scenario in the context of SCF, please refer to the end of Section 3.5.

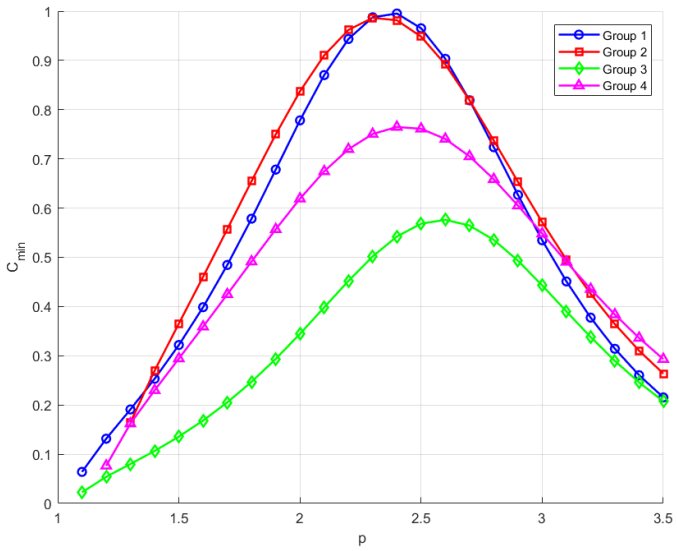

Figure 8. The relationship curves between $C_{\min}$ and p under different initial values.

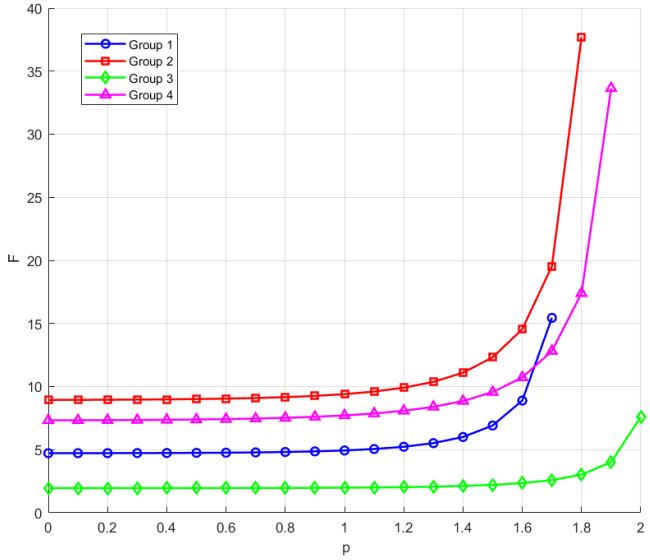

Figure 9. The relationship curves between $\mathcal{F}$ and p under different initial values.

4.4. The effect of α on τ_0

In this section, we examine how τ_0 varies as α changes. Before proceeding, we first recall the derived equations (3.10) and (3.11):

$$\tau_0 = \frac{1}{\omega_0}\arccos\left(-\frac{G_1G_3 + G_2G_4}{G_3^2 + G_4^2}\right), \quad \frac{d\tau_0}{d\alpha} = \frac{-\frac{1}{\sqrt{1-U^2}}\frac{\partial U}{\partial \alpha}\omega_0 - \frac{d\omega_0}{d\alpha}\arccos U}{\omega_0^2}.$$

Tracing back to their origins, G_1, G_2, G_3, G_4, and U are all determined by the parameters β, γ, ε, μ, Λ, and p.

Next, we set the relevant parameters:

$$\Lambda = 0.085, \quad \beta = 0.25, \quad \mu = 0.048, \quad \varepsilon = 0.3, \quad \gamma = 0.1, \quad p = 1.$$

The parameters ω and τ_0 are determined following the method described in Section 4.3. In computing the required partial derivatives $\frac{\partial G}{\partial \alpha}$ and $\frac{\partial G}{\partial \omega}$, a central difference scheme with a step size of $h = 10^{-6}$ is employed.

Following this, numerical simulations were carried out in MATLAB, and we present the following results:

Since the results presented in Figures 10 and 11 are essentially equivalent, we select Figure 11 for analysis. Figure 11 shows that as the fractional order α increases, the critical time delay τ_0 corresponding to the Hopf bifurcation decreases. In the context of SCF, a larger α indicates weaker memory effects in enterprise decision-making, meaning firms rely primarily on the most recent information while historical events exert limited influence. While this mode enables rapid responses, it undermines system stability. Moreover because enterprises depend heavily on real-time information, any delay in information transmission or evaluation quickly renders the decision-making basis outdated, potentially leading to misjudgments. Consequently, the critical time delay τ_0 that the decision-making process can tolerate becomes smaller. Once the evaluation delay τ exceeds τ_0, rapid decisions based on outdated information generate erroneous feedback, driving blockchain adoption rates into oscillations—manifested as the market swinging repeatedly between surges and retreats.

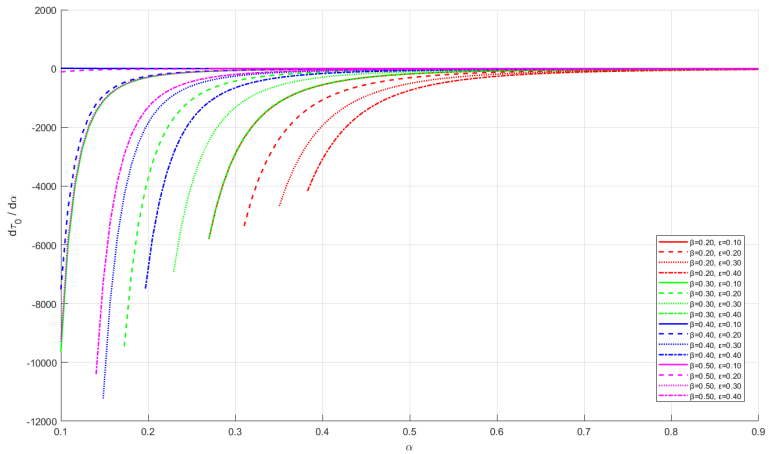

Figure 10. Variation of $\frac{d\tau_0}{d\alpha}$ with α.

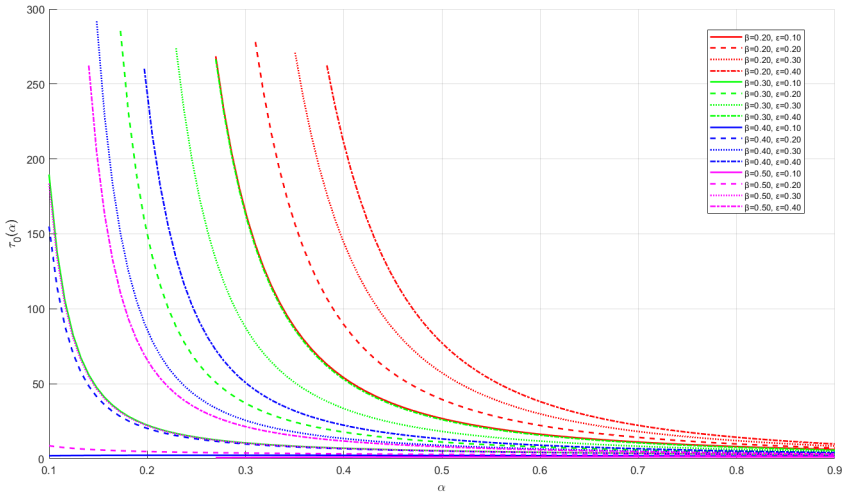

Figure 11. Variation of tau_0 with α.

Conversely, when α is smaller, enterprise decisions exhibit pronounced historical dependence, with current judgments moderated by past experience. This strong memory effect, while possibly slowing the decision-making pace, provides inertial stability to the system: Even in the presence of information delays, enterprises do not react sharply to outdated signals because decision weights are smoothed by historical experience. Hence, the system can tolerate longer evaluation cycles, i.e., it possesses a larger τ_0.

It is noteworthy that τ_0 declines relatively rapidly in the initial stage and then gradually levels off. Mapping this to the decision-making context of SCF, the rapid initial decline of τ_0 indicates that when enterprise decisions shift from strong reliance on historical experience (low α) toward greater consideration of recent information, the system's tolerance for evaluation delays decreases sharply. This occurs because once the decision-making mechanism begins to incorporate recent information, even to a modest extent, it significantly alters the stability maintained by long-term historical inertia, rendering the system more vulnerable to time delays. Hence, τ_0 drops quickly in this phase.

When the decision-making pattern heavily depends on real-time information (high α), further shortening the memory span (increasing α) brings about less noticeable changes in behavioral patterns, and its destabilizing effect on the system correspondingly diminishes. At this stage, system stability is predominantly governed by classic delay-driven mechanisms, leaving limited room for improvement. Consequently, the change in τ_0 tends to flatten.

4.5. Sensitivity analysis

To verify the reliability of the model's conclusions in realistic scenarios, we carry out sensitivity analysis on key parameters. The parameter settings are consistent with those in Section 4.2. Using Monte Carlo simulation, we examine the global stability of the model under simultaneous perturbations of multiple parameters. A ±10% uniformly distributed random perturbation is applied to the four key parameters α, β, τ, and p with 1,000 independent simulation runs. In all simulated cases, the basic reproduction number R_0 remains greater than 1, ensuring the universal existence of the positive

equilibrium. The results are as follows:

In Figure 12, the horizontal axis shows the values of I^*, and the vertical axis represents the frequency of each value. The blue dashed line denotes the baseline theoretical value of I^*, while the red solid line indicates the mean of all simulation results. The results show that I^* exhibits a multimodal distribution within the range of 0.87–0.99, with the simulated mean being highly consistent with the baseline value, demonstrating the good robustness of the model under parameter uncertainty.

In Figure 13, the horizontal axis represents the percentage change in I^* under ±10% parameter perturbations, and the vertical axis lists the model parameters. The blue bars denote the total range of I^* changes caused by each parameter, while the red and green triangles indicate the changes in I^* when parameters are decreased or increased by 10%, respectively. The results show that β is the most sensitive parameter to I^*, followed by ε and τ, whereas α and p have negligible effects.

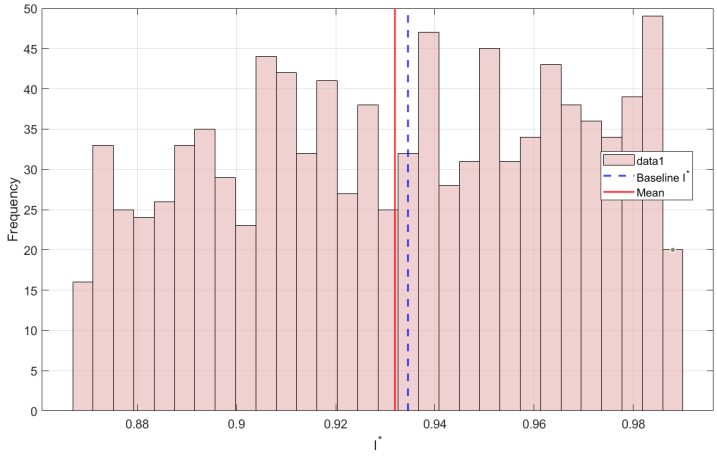

Figure 12. Frequency distribution of I^* from Monte Carlo simulations.

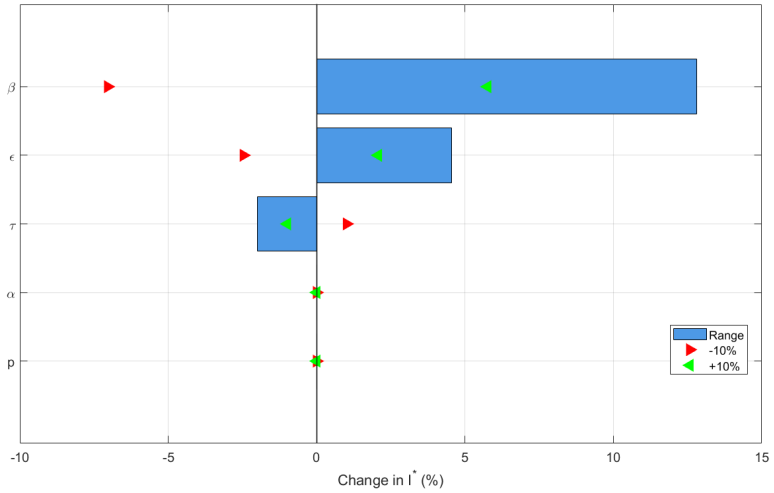

Figure 13. Tornado plot for sensitivity analysis of I^*.

Comprehensive analysis shows that the model exhibits strong robustness under parameter uncertainty. As for the non-monotonic relationship between p and $C_{\min}$, and the negative correlation between τ_0 and α under parameter perturbations, their sensitivity analyses are essentially captured in the results presented in Sections 4.3 and 4.4.

5. Conclusions

In this study, we introduce a novel fractional-order delayed SEIR model to examine the diffusion dynamics of BCT in SCF. The framework incorporates enterprises' sensitivity to information sharing as a key parameter and accounts for memory effects and time delays inherent in technology adoption processes. Theoretical analysis demonstrates that when $R_0 > 1$, the system exhibits a unique positive equilibrium, enabling sustained adoption. However, this endemic state can become destabilized by Hopf bifurcations induced by prolonged evaluation periods, resulting in oscillatory fluctuations in adoption rates. Theoretical derivation and numerical simulations reveal a negative correlation between the fractional order α and the system's stability threshold τ_0. A larger α corresponds to a smaller maximum tolerable security assessment delay τ_0, indicating that system stability becomes more sensitive and vulnerable to delays. Conversely, a smaller α endows the system with stronger inertial stability, enabling it to withstand longer evaluation cycles without losing stability. This finding profoundly illustrates how corporate decision-making patterns fundamentally shape the stability boundary of the technology diffusion ecosystem.

Furthermore, our findings reveal a fundamental duality in BCT diffusion. The information sharing sensitivity index p exerts a non-monotonic effect on the minimum wave speed of technology propagation, indicating the existence of an optimal range for diffusion velocity. Furthermore, increased sensitivity consistently amplifies the final adoption scale, underscoring its critical role in determining market penetration. These insights inform the design of phased implementation strategies. The early stage should prioritize establishing robust information-sharing infrastructure, while the later stage requires careful parameter calibration to maintain system stability and maximize adoption. Thus, we recommend that regulatory bodies or industry alliances establish a "tiered and classified information disclosure" standard. This standard would set varying scopes of data sharing and encryption levels according to data sensitivity. For example, basic transaction information could be mandated for shared access on-chain, while core financial details may be protected via permissioned access or similar technologies. This approach ensures necessary transparency while preventing excessive exposure of sensitive data. For industries with weak memory effects, it is advisable to promote the use of Service Level Agreements and standardized smart contract templates on supply chain finance blockchain platforms. This can significantly reduce the complexity and time required for contract negotiations.

Despite its contributions, this study has several limitations that warrant further investigation. While we introduce and analyze the impact of the information sharing sensitivity index p, its precise quantification remains unaddressed. In future studies, researchers could rigorously determine its empirical value. Here, we propose a conceptual approach. p can be quantified through a questionnaire survey administered to enterprises. The questionnaire can be designed with Likert-scale items to measure the willingness or concern of enterprises regarding "sharing transaction data", "disclosing credit information", and "making operational processes public" when considering blockchain adoption. By conducting principal component analysis or factor analysis on the scale scores, a composite

index reflecting information sharing sensitivity can be derived. Furthermore, p is expected to vary across different industries. For instance, in the financial services sector, due to stringent regulatory requirements and high data sensitivity, p is generally anticipated to be below 1 (indicating a tendency toward information damping). In contrast, in standardized manufacturing, where supply chain collaboration demands are strong and data standardization is high, p may approach or exceed 1 (reflecting a tendency toward positive feedback). Moreover, direct measurement of such indices remains scarce in the literature. This, researchers could focus on calibrating the specific range of p. Additionally, the coupling effects of fractional order (α), time delay (τ), and information-sharing sensitivity(p) are not fully explored. As such, researchers could examine how variations in α and τ influence diffusion speed and final adoption scale. Furthermore, in practice, core enterprises may exhibit a longer τ due to their abundant resources and complex decision-making processes, while small and medium-sized enterprises, characterized by flexible decision-making, are likely to have a shorter τ. Additionally, researchers could adopt a distributed time-delay approach. Moreover, we have not systematically examined the impact of different supply chain topologies on technology diffusion pathways. Thus researchers could integrate industry case studies or simulation data to further explore the interaction effects between network structural characteristics and key model parameters, thereby enhancing the model's explanatory power and predictive accuracy across industrial contexts. Moreover, researchers could investigate the design of incentive mechanisms aimed at enhancing inter-firm information sharing, further promoting blockchain adoption in SCF.

Author contributions

Peng Wan, Sumei Pan: Writing-original draft, methodology; Shujian Ma, Jun Wang, Minyi Xu: Visualization, conceptualization, project administration; Jiangwen Ju: Validation. All authors have read and approved the final version of the manuscript for publication.

Use of Generative-AI tools declaration

The authors declares they have used Artificial Intelligence (AI) tools in the creation of this article. The manuscript's English language was checked and polished using ChatGPT to improve grammar, spelling, clarity, and academic tone. Moreover, the AI tool DeepSeek was employed to assist in verifying the correctness of Eqs (3.2) and (3.11) after their manual derivation.

Acknowledgments

Comments and suggestions of referees and the editor were very helpful in improving the paper, and all individuals included in this section have consented to the acknowledgment. Moreover, they appreciate the National Social Science Foundation of China (grant number 20GBL009).

Conflict of interest

All authors declare no conflicts of interest in this paper.

References

1. S. Wang, M. Zhou, S. Xiang, Blockchain-enabled utility optimization for supply chain finance: An evolutionary game and smart contract based approach, *Mathematics*, **12** (2024), 1243. https://doi.org/10.3390/math12081243
2. Y. Teng, S. Ma, Q. Qian, G. Wang, SEIR-diffusion modeling and stability analysis of supply chain finance based on blockchain technology, *Heliyon*, **10** (2024), e24981. https://doi.org/10.1016/j.heliyon.2024.e24981
3. Q. Zhu, R. Zong, M. Xu, Three-party stochastic evolutionary game analysis of supply chain finance based on blockchain technology, *Sustainability*, **15** (2023), 3084. https://doi.org/10.3390/su15043084
4. S. Li, S. Qu, The three-level supply chain finance collaboration under blockchain: Income sharing with Shapley value cooperative game, *Sustainability*, **15** (2023), 5367. https://doi.org/10.3390/su15065367
5. E. Hofmann, O. Belin, *Supply chain finance solutions*, SpringerBriefs in Business, Springer, 2011, 13–70. https://doi.org/10.1007/978-3-642-17566-4
6. P. K. Wan, L. Huang, H. Holtskog, Blockchain-enabled information sharing within a supply chain: A systematic literature review, *IEEE Access*, **8** (2020), 49645–49656. https://doi.org/10.1109/ACCESS.2020.2980142
7. M. Vosooghidizaji, A. Taghipour, B. Canel-Depitre, Supply chain coordination under information asymmetry: A review, *Int. J. Prod. Res.*, **58** (2020), 1805–1834. https://doi.org/10.1080/00207543.2019.1685702
8. F. Caniato, L. M. Gelsomino, A. Perego, S. Ronchi, Does finance solve the supply chain financing problem? *Supply Chain Manag.*, **21** (2016), 534–549. https://doi.org/10.1108/SCM-11-2015-0436
9. T. Beck, A. Demirguc-Kunt, Small and medium-size enterprises: Access to finance as a growth constraint, *J. Bank. Financ.*, **30** (2006), 2931–2943. https://doi.org/10.1016/j.jbankfin.2006.05.009
10. G. F. Qiu, Y. Zhang, C. Wang, Study on information asymmetry and the risks initiated by it in the supply chain finance, *Appl. Mech. Mat.*, **2948** (2014), 2827–2831. https://doi.org/10.4028/www.scientific.net/AMM.496-500.2827
11. M. Ni, W. Bo, X. Qin, F. Yao, CSR input and recycling decisions for closed-loop supply chain with asymmetric demand information, *Systems*, **13** (2025), 432. https://doi.org/10.3390/systems13060432
12. M. Abdulaziz, D. Sackmann, A. Fiedler, S. Rhein, M. Alghababsheh, Determinants of information asymmetry in agri-food supply chains, *Int. J. Logist. Manag.*, **36** (2025), 259–289. https://doi.org/10.1108/IJLM-08-2023-0330
13. S. D. Kotey, E. T. Tchao, A. S. Agbemenu, A. R. Ahmed, E. Keelson, A framework for full decentralization in blockchain interoperability, *Sensors*, **24** (2024), 7630. https://doi.org/10.3390/s24237630
14. S. H. Bae, S. Saberi, M. Kouhizadeh, J. Sarkis, Examining blockchain's role in supply chain finance structure and governance, *Int. Rev. Financ. Anal.*, **99** (2025), 103955. https://doi.org/10.1016/j.irfa.2025.103955

15. S. S. Liu, B. J. Ma, W. Zhang, E. T. C. Cheng, X. W. Li, C. T. Ng, Eliminating information asymmetry in supply chains: Blockchain-driven or not, *Transport. Res. E-Log.*, **201** (2025), 104208. https://doi.org/10.1016/j.tre.2025.104208

16. L. Guo, J. Chen, S. Li, Y. Li, J. Lu, A blockchain and IoT-based lightweight framework for enabling information transparency in supply chain finance, *Digit. Commun. Netw.*, **8** (2022), 576–587. https://doi.org/10.1016/j.dcan.2022.03.020

17. S. Saberi, M. Kouhizadeh, J. Sarkis, L. Shen, Blockchain technology and its relationships to sustainable supply chain management, *Int. J. Prod. Res.*, **57** (2019), 2117–2135. https://doi.org/10.1080/00207543.2018.1533261

18. T. M. Choi, Blockchain-technology-supported platforms for diamond authentication and certification in luxury supply chains, *Transport. Res. E-Log.*, **128** (2019), 269–290. https://doi.org/10.1016/j.tre.2019.05.011

19. A. K. Jha, S. Kumar, A. Jain, Don't overdo it with blockchain—understanding the impact of blockchain on users' security perception, *Mark. Intell. Plan.*, **43** (2025), 777–801. https://doi.org/10.1108/MIP-10-2023-0555

20. R. Beck, M. Avital, M. Rossi, J. B. Thatcher, Blockchain technology in business and information systems research, *Bus. Inform. Syst. Eng.*, **59** (2017), 381–384. https://doi.org/10.1007/s12599-017-0505-1

21. L. W. Wong, L. Y. Leong, J. J. Hew, G. W. H. Tan, Time to seize the digital evolution: Adoption of blockchain in operations and supply chain management among Malaysian SMEs, *Int. J. Inform. Manag.*, **52** (2020), 101997. https://doi.org/10.1016/j.ijinfomgt.2019.08.005

22. E. Kiesling, M. Günther, C. Stummer, L. M. Wakolbinger, Agent-based simulation of innovation diffusion: A review, *Cent. Eur. J. Oper. Res.*, **20** (2012), 183–230. https://doi.org/10.1007/s10100-011-0210-y

23. R. Peres, E. Muller, V. Mahajan, Innovation diffusion and new product growth models: A critical review and research directions, *Int. J. Res. Market.*, **27** (2010), 91–106. https://doi.org/10.1016/j.ijresmar.2009.12.012

24. J. Ding, S. Liu, Y. Lv, J. Zhang, Q. Zhou, Research on the diffusion and control of unsafe behaviors among chemical industry park enterprises based on the SEIR evolutionary game model, *J. Loss Prevent. Proc.*, **92** (2024), 105456. https://doi.org/10.1016/j.jlp.2024.105456

25. S. A. Delre, W. Jager, T. H. A. Bijmolt, M. A. Janssen, Targeting and timing promotional activities: An agent-based model for the takeoff of new products, *J. Bus. Res.*, **60** (2017), 826-835. https://doi.org/10.1016/j.jbusres.2007.02.002

26. S. Paul, A. Mahata, M. Karak, S. Mukherjee, S. Biswas, B. Roy, A fractal-fractional order susceptible-exposed-infected-recovered (SEIR) model with Caputo sense, *Healthcare Anal.*, **5** (2024), 100317. https://doi.org/10.1016/j.health.2024.100317

27. J. Zeng, X. Chen, L. Wei, D. Li, Bifurcation analysis of a fractional-order eco-epidemiological system with two delays, *Nonlinear Dynam.*, **112** (2024), 22505–22527. https://doi.org/10.1007/s11071-024-10184-y

28. V. Kumar, N. Kumari, Exploring the impact of time delay with fractional derivative and diffusion in a three-species food chain model, *Iran. J. Sci.*, 2025. https://doi.org/10.1007/s40995-025-01886-y

29. S. Soulaimani, A. Kaddar, F. A. Rihan, Analysis of a fractional endemic SEIR model with vaccination and time delay, *Eur. Phys. J. Spec. Top.*, **234** (2024), 1–17. https://doi.org/10.1140/epjs/s11734-024-01267-3

30. W. Liu, H. W. Hethcote, S. A. Levin, Dynamical behavior of epidemiological models with nonlinear incidence rates, *J. Math. Biol.*, **25** (1987), 359–380. https://doi.org/10.1007/BF00277162

31. H. R. Thieme, X. Q. Zhao, Asymptotic speeds of spread and traveling waves for integral equations and delayed reaction diffusion models, *J. Differ. Equations*, **195** (2003), 430–470. https://doi.org/10.1016/S0022-0396(03)00175-X

32. B. Guenad, R. Darazi, S. Djilali, I. Alraddadi, Traveling waves in a delayed reaction–diffusion SIR epidemic model with a generalized incidence function, *Nonlinear Dynam.*, **113** (2024), 1–21. https://doi.org/10.1007/s11071-024-10413-4

33. J. D. Murray, *Geographic spread and control of epidemics*, In: Murray, J.D. (eds) Mathematical Biology, Interdisciplinary Applied Mathematics, Springer, **18** (1993), 661–721. https://doi.org/10.1007/0-387-22438-6_13

34. I. Podlubny, *Fractional differential equations*, Academic Press, 1999.

35. W. van Saarloos, Front propagation into unstable states, *Phys. Rep.*, **386** (2003), 29–222. https://doi.org/10.1016/j.physrep.2003.08.001

36. H. J. Haubold, A. M. Mathai, R. K. Saxena, Mittag-Leffler functions and their applications, *J. Appl. Math.*, **2011** (2011), 298628. https://doi.org/10.1155/2011/298628

37. E. Badakhshan, D. Ivanov, Integrating simulation and decision trees through blockchain-enabled data sharing to prevent the cash flow bullwhip effect in supply chains, *Ann. Oper. Res.*, 2025. https://doi.org/10.1007/s10479-025-06858-4

AIMS Press